ELECTRODEPOSITION OF NICKEL COMPOSITE COATINGS

By

TUSHAR BORKAR

Bachelor of Engineering in Mechanical Engineering

Mumbai University

Mumbai, Maharashtra, INDIA

2007

Submitted to the Faculty of the
Graduate College of the
Oklahoma State University
in partial fulfillment of
the requirements for
the Degree of
MASTER OF SCIENCE
December, 2010

ELECTRODEPOSITION OF NICKEL COMPOSITE

COATINGS

Thesis Approved:

Dr. Sandip P. Harimkar

Thesis Adviser

Dr. Jay C. Hanan

Dr. Raman P. Singh

Dr. Mark E. Payton

Dean of the Graduate College

ACKNOWLEDGEMENTS

I would like to express my heartfelt gratitude to my advisor, Dr. Sandip P. Harimkar for his guidance, enthusiasm, patience, motivation, and enormous knowledge throughout my master's study. He is always encouraging me by his innovative way of thinking and positive attitude towards research work. This project has completed only due to his enthusiasm and immense input of ideas. I could not have imagined a better advisor than him for my Master's study, without him I would have been lost. I would like to thank Dr. Jay Hanan and Dr. Raman Singh for being in my thesis committee, for providing helpful suggestions and for their encouragement. I would like to thank Dr. Kaan Kalkan for allowing me to use his Raman Spectroscopy instrument for my experiments.

I would also like to acknowledge my research group mates Ashish Singh, Vineet Yadav, Vamsi Karthik, and Mrinalini Mulukutla for the stimulating discussions, for their help during my Master's studies and making research lab being a nice place to work. I would like to thank my friends Ameya and Suyog for helping me in dealing with stress and giving emotional support throughout my studies.

Last but not the least, I would like to give deepest thanks to my parents Murlidhar and Mangal Borkar and grandparents Laxman and Vithabai Borkar for their love and spiritual support throughout my life without which I would not have complete this work.

TABLE OF CONTENTS

Chapter Page

Chapter Page

Chapter Page

LIST OF TABLES

Table Page

LIST OF FIGURES

Figure Page

Chapter 1:

Figure Page

Figure Page

Chapter 3:

Figure Page

Figure Page

Figure Page

CHAPTER 1

INTRODUCTION

1.1 Introduction

Electrodeposition is one of the most technologically feasible and economically superior techniques for producing metal matrix composites. DC (direct current) electrodeposition method is widely used for fabrication of metal matrix coatings from many decades [1]. Recently, PC (pulse current), and PRC (pulse reverse current) electrodeposition methods have received much attention to improve mechanical and corrosion properties of coatings [2, 3]. In this work, Nickel composite coatings (Ni-Al_2O_3, Ni-SiC, and Ni-ZrO_2) were successfully synthesized by DC, PC, and PRC techniques to study effect of electrodeposition methods on microstructure, mechanical, and tribological behavior. Ni-CNT composite coatings were also fabricated by pulse electrodeposition method to investigate CNT reinforcement effect on mechanical and tribological property. Ni-Al_2O_3 composites coatings were deposited to analyze effect of nanoparticles on properties of composite coatings. This chapter provides literature review on different types of electrodeposition methods, co-deposition processes and nickel composite coatings.

1.2 Electrodeposition Process

Electrodeposition is simple and economical technique for the production of dense metallic nanocrystals [4]. DC, PC, and PRC electrodeposition methods used to fabricate metallic coatings. Qu *et al.* deposited nickel coatings by DC and PC electrodeposition method and observed significant improvement in hardness in PC electrodeposited coatings than DC electrodeposited nickel coatings [5]. Tao *et al.* fabricated Nanocrystalline copper coatings to study tribological and mechanical properties of Nanocrystalline copper coatings [6]. Copper coatings deposited by PC electrodeposition technique have higher hardness and wear resistance compared to DC electrodeposited coatings. Pure nickel coatings deposited by PC and PRC techniques have better corrosion resistance than DC electrodeposited nickel coatings [2]. This chapter provides brief overview on DC, PC, and PRC electrodeposition methods.

1.2.1 DC (Direct Current) Electrodeposition

In the conventional DC electrodeposition, only one parameter i.e. current density can be varied. Fig. 1.1 shows typical waveform of current v/s deposition time for DC electrodeposition. Duty cycle (i.e. ratio of current ON time to total time) is 100% in DC electrodeposition. Therefore average current density (Avg. current density equals to duty cycle X Peak current density) which equals to peak current density.

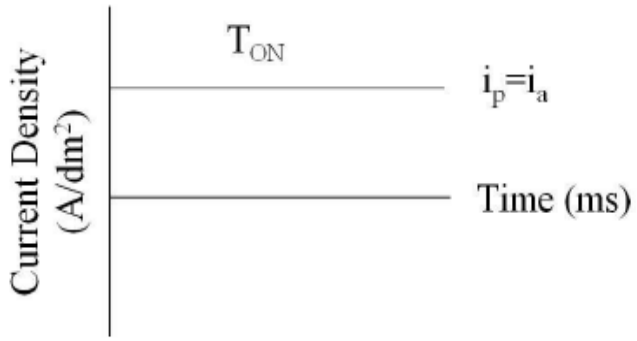

Fig. 1.1 *Typical direct current waveform.*

1.2.2 PC (Pulse Current) and PRC (Pulse Reverse Current) Electrodeposition

Pulse Electrodeposition (PED) brings a new era in the electrodeposition of metals, alloys, and metal matrix composites (MMCs). Compared to the conventional direct current (DC) electrodeposition, there is much more flexibility in the pulse electrodeposition technique in terms of varying basic electrodeposition parameters such as peak current density (i_p), pulse current on-time (T_{ON}), and pulse current off-time (T_{OFF}) resulting in unique combination of composition and microstructure in deposited coatings. The average current density (i_a) can be obtained by a number of combinations of different peak current densities, pulse current on-time, and pulse current off-time [7]. Also, pulse electrodeposition current can be efficiently alternated between two different values resulting into a series of pulses of equal amplitude, duration, and polarity separated by zero current [8]. A typical pulse current waveform where current is alternated between a positive current value (i_p) applied for T_{ON} time and zero current value (0) applied for T_{OFF} time is presented in Fig. 1.2. Concepts of pulse and pulse reverse techniques [8]:

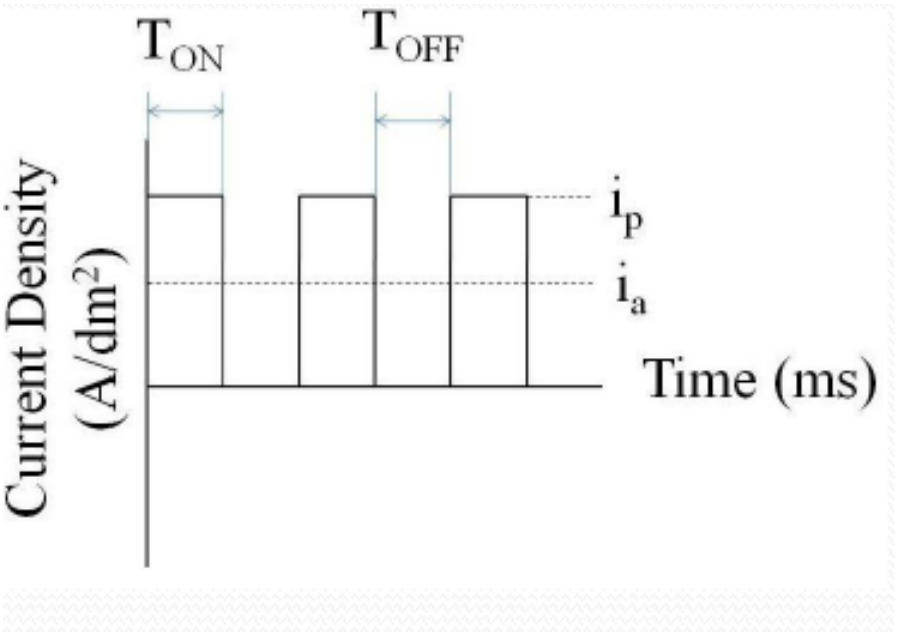

Fig. 1.2 *Typical pulse current waveform.*

- During T_{OFF} time in pulse electrodeposition, the electric double layer which is formed around the cathode discharges resulting in the passage of ions through the double layer on cathode surface, whereas in DC electrodeposition, this double layer obstructs the ions from reaching the cathode surface.
- During electrodeposition, high current density areas in the electrolyte bath are more depleted of ions than that of low current density areas. During T_{OFF} time, ions migrate to these depleted areas. So that, more evenly distributed ions are available for deposition onto the part when T_{ON} pulse occurs.

Pulse electrodeposition allows synthesis of coatings with controlled coating thicknesses as well as compositions and microstructures of the coatings by regulating pulse parameters. PC and PRC electrodeposition techniques have following advantages and disadvantages over DC electrodeposition technique [7, 8]

Advantages:

- Limiting current density significantly increases by replenishing metal ions in the diffusion layer only during off time.
- Flexibility in pulse parameters reduces the process limitations.
- Fine grained deposit with lower porosity and reduced stress.
- Improves adhesion of deposit, creates uniform thickness.
- Higher rate of deposition improvements in physical and mechanical properties.

Disadvantages:

- Pulse generators are expensive than DC unit.
- This technique needs proper planning in advance with series of procedures in order to attain better results.

1.3 Electrodeposition of composite Coatings (Co-deposition Process)

Co-deposition is process of incorporating fine particles of metallic, non-metallic compounds, or polymers from an electrolytic or an electroless bath in the electroplated layer to improve material properties such as hardness, wear resistance, corrosion resistance, lubrication, yield, tensile, and fracture strength [9-21]. The well-dispersed nanoparticles in the composites not only improving mechanical properties but also find suitable applications in microdevices [22, 23]

1.3.1 Theory/ Mechanisms of Co-deposition Process

Physical dispersion of particles in the electrolyte and electrophoretic migration of particles are two common processes involved in co-deposition of particles into metal deposite [17]. Composite electroplating is a method of co-depositing micron, sub-micron size particles of metallic, non-metallic compounds into plated layer. There are two models developed for composite electrodeposition by Guglielmi and Kurozaki.

According to Guglielmi's model, composite electroplating takes place in two steps. During electrodeposition, solid particles are surrounded with cloud of adsorbed ions and these particles are weakly adsorbed at cathode surface by Vander Walls forces when they approach the cathode in the first step. And in the second step, loosely adsorbed particles get adsorbed strongly on cathode surface by Coulomb force and consequently entrapped within metal matrix. The main drawback of this model is absence of mass transfer effect during electrodeposition process. [13, 24, 25]

Greatly accepted model is developed by Kurozaki which includes the transport of solid particles from the solution to the cathode surface by agitation [16, 25]. This model developed three step processes which include:

(1) Uniformly dispersed particles are transported to the electric double layer by mechanical agitation

(2) Charged particles are transported to cathode surface by electrophoresis

(3) Solid particles are adsorbed at cathode surface due to Coulomb force between particles and adsorbed anions. and finally incorporated into growing metal.

One of the common mechanism of co-deposition process consist of five consecutive steps [17] shown in Fig. 1.3. The regions include: formation of ionic clouds around the particles (bulk electrolyte, typical length in cm); convective movement toward the cathode (convection layer, typical length < 1 mm); diffusion through a concentration boundary layer (diffusion layer, typical dimensions of hundreds of μm); electrical double layer (typical dimensions of nm) followed by adsorption and entrapment of particles.

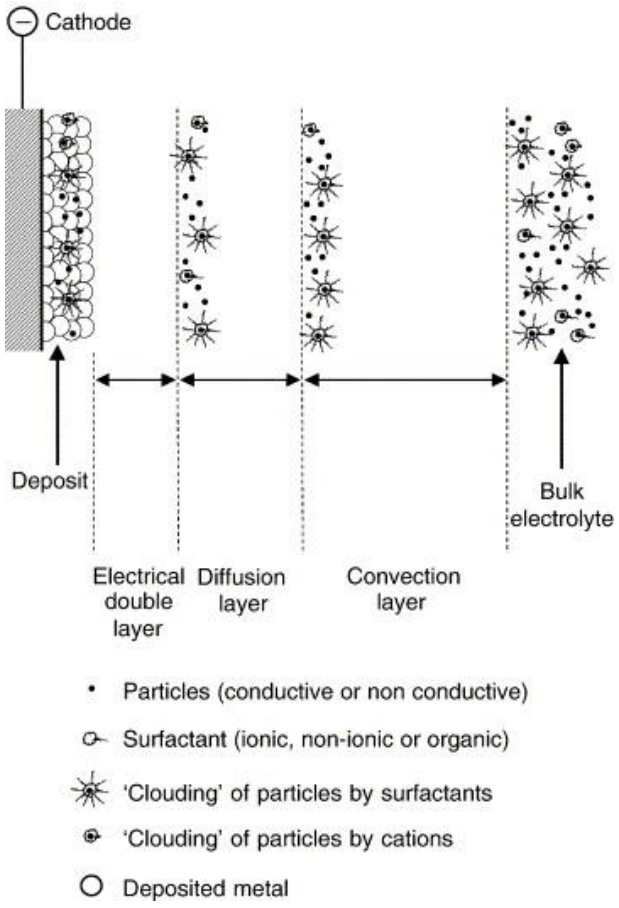

Fig. 1.3 *Mechanisms of particle codeposition into a metal deposit [17].*

Five consecutive steps of co-deposition mechanism are:

(1) Formation of ionic clouds on the particles

(2) Convection towards the cathode

(3) Diffusion through hydrodynamic boundary layer

(4) Diffusion through concentration boundary layer

(5) Adsorption at the cathode where particles are entrapped within metal deposit.

Particles dispersed in the electrolyte bath are in constant Brownian motion. Whenever two particles approach one another, their separation or agglomeration mainly depends on the existing energies between those particles. When attraction energy is larger than repulsion energy, particle agglomeration occurs and when repulsion energy is higher than attraction energy, particle separation occurs. The condition and nature of the system mainly determines the magnitude of net force for the production of agglomerated structures [13]. Therefore, knowledge of interfacial region structure is very important in understanding dispersion stability of solid particles with electrolyte.

1.3.2 Different Types of Composite Coatings

Varieties of composite coatings were deposited by reinforcing different nanoparticles (such as Al_2O_3, SiC, CNTs, ZrO_2, Si_3N_4, and WC) into metal matrix. Wang *et al.* deposited Al_2O_3-Cu(Sn), CaF_2-Cu(Sn), and talc-Cu(Sn) composite coatings to study mechanical and tribological behavior of composite coatings [26]. Al_2O_3-Cu(Sn)

composite coatings exhibited better hardness and wear resistance than other composite coatings due to high hardness of alumina nanoparticles. Arai *et al.* fabricated Cu-MWCNT composite coatings by electrodeposition method [27]. CNT reinforcement in the composite coatings significantly improved hardness and electrical as well as thermal conductivities of composite coatings. Rajiv *et al.* characterized corrosion behavior of CO-Si_3N_4 composite coatings [28]. CO-Si_3N_4 composite coatings showed better corrosion resistance as compared to pure CO coatings. Hashimoto and Abe characterized Zn-SiO_2 composites before and after corrosion test [29]. Zn-SiO_2 composites exhibited better corrosion resistance due to formation of protective corrosion products supported by SiO_2.

1.3.3 Effect of Pulse Parameters on Mechanical and Tribological Properties of Composite Coatings

The structure and properties of composite coatings depend not only on concentration, size, distribution, and nature of reinforced particles, but also on electroplating parameters (i.e. current density, duty cycle, and frequency). Among these factors current density is one of the most important parameters. In this section, effects of these parameters on mechanical properties of composite coatings reviewed in detail.

1.3.3.1 Current Density

Particles reinforcement in the composite coatings varies with current density. At first, incorporation increases sharply at the beginning with increase in current density till it

reaches maximum value followed by sharp decrease. Therefore, hardness of composite coatings mainly increases due to the combined effect of both grain refining as well as of dispersive strengthening [30-32]. When electroplating at lower current densities, nickel ions dissolved from anode (i.e. nickel) are transported at low rate and hence there is insufficient time for these ions to absorb on particles resulting in weak Coulomb force between anions adsorbed on particles leading to lower concentration of electrodeposited particles in the composite coatings. On the other hand, at higher current densities, nickel ions dissolved from anode are transported faster than particles by the mechanical agitation which causes a decrease in codeposition of particles as well as hardness of composite coatings. Therefore, selection of optimum current density is important to enhance the concentration of particles in the composite coatings [25, 33]. Many researchers found similar results, when electrodeposited at different current densities in terms of improvement in hardness as well as incorporation of particles in the composite coatings [16, 17, 34-38]. Reinforcement of nanoparticles into metal matrix not only restrains the grain growth but also reduces the plastic deformation of metal matrix by combined effect of grain refining and dispersion strengthening resulting in significant increase in hardness of composite coatings [33].

1.3.3.2 Pulse Frequency

Pulse frequency plays an important role in the reinforcement of nanoparticles in composite coatings. According to Lajevardi *et al*. microhardness as well as codeposition of particles increases on variation of frequency from 0.1 Hz to 10 Hz and is followed by

sharp decrease from 10 Hz to 100 Hz frequency [33]. For frequencies below 10 Hz, reduction rate of metal ions is higher as compared to ions adsorbed on nanoparticles which reduce the nanoparticles content in the composite coating. At lower frequencies below 10 Hz, due to extensive OFF time, loosely adsorbed particles could be removed by hydrodynamic force. Therefore at 10 Hz frequency, there is reduction in OFF time which causes less loosely adsorbed particles could be detached. At very high frequency i.e. 100 Hz, content of nanoparticles in composite coating reduced because of the shorter OFF time is not sufficient to remove concentration gradient of nanoparticles adjacent to the cathode. Wear loss and microhardness of composite coatings significantly decreases when pulse frequency increase from 10 Hz to 1000 Hz. Significant adhesive wear observed at higher frequencies [9].

1.3.3.3 Duty Cycle

Influence of duty cycle on incorporated particles is more prominent than effect of pulse frequency [30]. Bahrololoom *et al.* as well as Lajevadi *et al.* concluded similar results on effect of duty cycle on hardness as well as on incorporated particles in the composite coatings. As duty cycle increases from 10 to 100% microhardness as well as incorporated particles decreases significantly. Lower duty cycle gives longer OFF time for arrival of nanoparticles at the double layer. Therefore more nanoparticles are reinforced in composite coatings at lower duty cycle and coatings become harder [32, 33]. The improvement in hardness at lower duty cycle is mainly due to grain refinement at pulse OFF-time longer than ON- time [39, 40].

1.4 Co-deposition of Nickel Composite Coatings

Nickel composite coatings usually deposited from Watts type or sulfamate bath containing nanoparticles (i.e. SiC [15, 16, 19-21], Al_2O_3 [9, 13], ZrO_2 [11, 12], TiO_2 [41], WC [10], SiO_2 [21], and CNTs [42, 43]) are in suspension. The improvement in hardness is due to the combination of both rule of mixture and dislocation pinning effect [44]. Additions of nanoparticles mainly inhibit grain growth and promote nucleation sites.

1.4.1 Nickel Composite Coatings-A Review

1.4.1.1 Ni-Al_2O_3 Composite Coatings

Nickel is a corrosion resistant metal. Incorporation of alumina nanoparticles in nickel composite coatings significantly improves hardness and corrosion as well as wear resistance. Higher concentration and uniform dispersion of particles in metal matrix improves tribological properties and oxidation resistance of composite coatings. Saha *et al.* observed effect of current density on the electrodeposited Ni-Al_2O_3 composite coatings [25]. Microhardness and wear resistance of composite coatings showed significant improvement at current density of 0.01 A/cm^2. The significant improvement in hardness of these composite coatings was mainly due to combine effect of dispersion strengthening as well as grain refinement. Abrasive strength of Ni-alumina composite coatings was reported to be 57 MPa. Ferkel *et al*. deposited nickel composite coatings by varying alumina content in electrolyte bath [40]. Composite coatings exhibited maximum hardness for 8 g/L alumina concentrating in the electrolyte. Qu *et al.* found microhardness of composite coatings was 346 HV deposited at peak current density of

1.5 A/dm2, 50 % duty cycle and frequency of 5.6 Hz which was higher than that of pure nickel coatings is 192 HV [23].

Bahrololoom *et al.* analyzed thoroughly the influence of pulse plating parameters on the hardness and wear resistance of nickel-alumina composite coatings [30]. Hardness and wear resistance of composite coatings as well as microstructure and surface morphology were strongly influenced by current density. Fig. 1.4 shows that the hardness of composite coatings decreases with increase in current density which is in good agreement with the results obtained by many researchers.

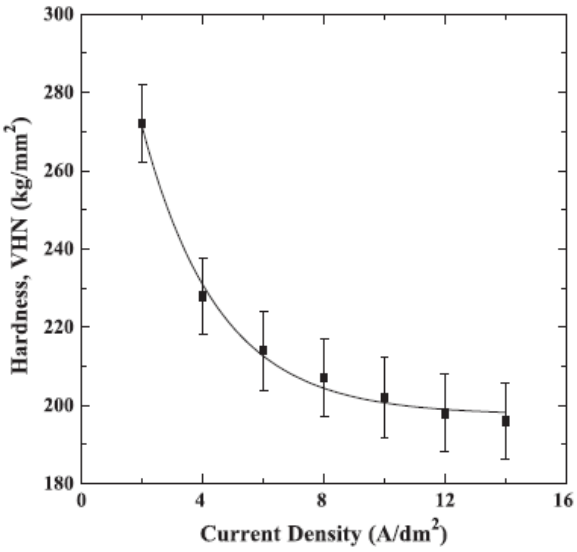

Fig. 1.4 *Effect of direct current density on the hardness of nickel–alumina composite coatings, electrodeposited from a bath containing 80 g/L alumina [30].*

Fig. 1.5 shows effect of duty cycle and frequency on hardness of composite coatings. At lower duty cycle and frequency, composite coatings show maximum hardness which sharply decrease with increase in duty cycle and pulse frequency. Lower duty cycle and frequency means longer OFF-time which gives more chance for alumina particles to

arrive at the double layer. Influence of duty cycle is more prominent than influence of frequency on incorporation of alumina particles.

Chen *et al.* studied influence of pulse frequency on microstructure and wear resistance of nickel-alumina composite coatings [45] . At lower frequencies, composite coatings exhibited better hardness and wear resistance compared to higher frequencies. Due to presence of adhesive wear, wear resistance of composite coatings largely influenced by microstructure and less influenced by reinforced alumina particles.

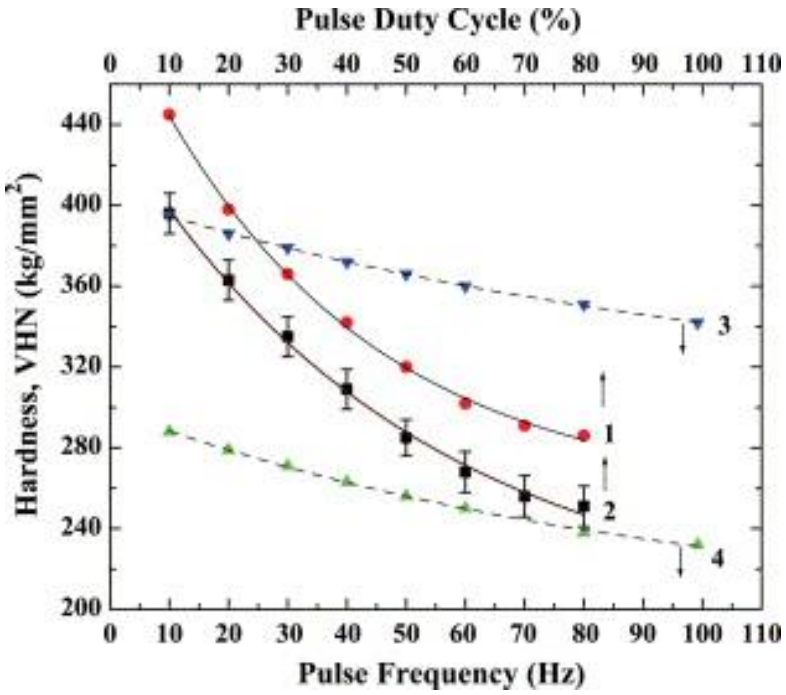

Fig. 1.5 *Effects of pulse duty cycle (solid lines) and frequency (dash lines) on the hardness of nickel–alumina composite coatings electrodeposited from a bath containing 80 g/L alumina (5 μm particle size), at a pulse current density of 5 A/dm^2 [30].*

1.4.1.2 Ni-SiC Composite Coatings

Ni-SiC composite coatings are widely used for protection of friction parts due to their high wear resistance and low cost of ceramic powder. Zimmerman *et al.* synthesized Ni-SiC composite coatings by pulse electrodeposition allowing high over potential and low surface diffusion rates resulting in formation of new nuclei [19]. The composite coatings exhibited four times hardness than annealed nickel and two time hardness than regular grain size nickel matrix. Vaezi *et al.* evaluated wear and corrosion resistance of Ni-SiC composite coatings fabricated using electrodeposition method [46]. The microhardness, wear as well as corrosion resistance of composite coatings increased with increasing SiC content in the plating bath. The increase in microhardness and wear resistance was mainly due to incorporated SiC particles which restrain grain growth as well as plastic deformation and promotes the grain refining and dispersive strengthening. These effects became stronger with increasing SiC content in the electrolyte. Nickel composite coatings showed wide passive region and smaller passive current density than pure nickel coatings. The reinforced SiC particles act as a physical barrier to initiation and development of defect corrosion resulting in improvement in corrosion resistance of composite coatings. Hou *et al.* studied wear behavior of electrodeposited Ni-SiC composites [22]. Nickel composite coatings exhibited maximum hardness and wear resistance compared to pure nickel coatings. For 2 vol.% Ni-SiC composite coatings showed maximum fluctuation in coefficient of friction due to presence of severe abrasive wear. For 11.5 vol.% nickel composite coatings showed decrease in coefficient of friction due to low plowing grooves. Worn out material from rotating steel ring i.e. iron

oxide debris layer covered the worn surface and acts as a lubricant between contact surfaces and coefficient of friction decreases further.

Zimmerman *et al.* analyzed mechanical properties of Ni-SiC nanocomposites [20]. Nickel composites showed significant improvement in mechanical properties including hardness, yield, and tensile stress as compared to conventional nickel composites. Tensile strength of composites was four times higher than polycrystalline nickel and two times higher than conventional polycrystalline nickel composites. The improvement in hardness of composites wass mainly based on dispersion strengthening mechanism which is based on dislocation particle interaction.

1.4.1.3 Ni-ZrO_2 Composites Coatings

Nickel and Zirconia have good compatibility due to their similar thermal expansion coefficient and elastic modulus. Wang *et al.* fabricated Ni-ZrO_2 composite coatings by DC, PC, and PRC electrodeposition techniques for comparison [47]. The surface morphology of DC, PC, and PRC composite coatings is shown in Fig. 1. 6.

PC composite coatings showed smooth and compact micro-surface morphology compared to DC and PRC composite coatings. The PRC composite coatings showed maximum hardness due to combination of grain refinement by Hall-petch mechanism and dispersion strengthening by Orowan's mechanism. Hardness of composite coatings depends not only on reinforced particles but also on size and distribution of particles in matrix. Due to uniformly dispersed ZrO_2 particles in nickel matrix, PRC composite coatings showed lower wear loss than DC and PC composite coatings. Ding *et al.* performed Nanoindetation characterization of Ni-ZrO_2 composite coatings [11]. The

composite coatings found superior young's modulus and microhardness than pure nickel due to combine effect of Hall-petch and Orowan mechanisms. Banea analyzed tribocorrosion behavior of electrodeposited nickel-zirconia composite coatings [48]. The microhardness and tribocorrosion properties of composite coatings were significantly improved due to uniformly dispersed ZrO_2 particles reinforcement in the nickel matrix followed by combined effect of dispersion strengthening and structural modification.

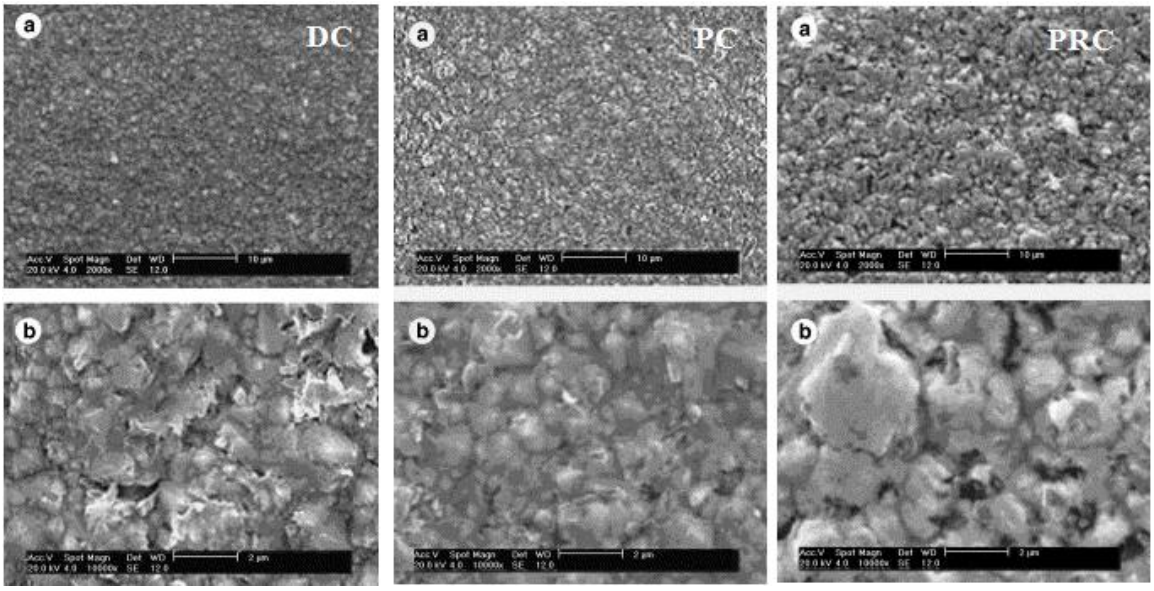

Fig. 1. 6 *Surface morphology of DC, PC, and PRC composite coatings [11].*

1.4.1.4 Ni-TiO_2 Composite Coatings

Metal matrix composites with TiO_2 reinforcement exhibit interesting photocatalytical behavior with significant improvement in mechanical properties. Ni-TiO_2 composite coatings are widely used in fuel cell applications particularly in electro-oxidation of

methanol. Baghery *et al.* characterized corrosion and wear performance of Ni-TiO_2 nanocomposite coatings [34]. Microhardness of Ni-TiO_2 composite coatings significantly improved than pure nickel coatings due to grain refinement strengthening and dispersion strengthening. The reinforced TiO_2 particles in nickel composite coatings reduced direct contact between abrasive surface and metal matrix. These separated particles act as solid lubricant between two wear surfaces. Therefore, Ni-TiO_2 composite coatings exhibited higher wear resistance mainly due to higher hardness and lower coefficient of friction. Presence of TiO_2 particles, act as a physical barrier to the initiation and development of defect corrosion and also it inhibits localized corrosion, resulting in improvement in corrosion resistance of nickel composite coatings. Lajevardi and Shahrabi studied effect of pulse parameters on properties of Ni-TiO_2 nanocomposite coatings [33]. Microhardness of composite coatings increased with increasing current density from 2 to 5 A/dm^2 and after that it decreased as current density increases. Microhardness and particle reinforcement in composite coatings found maximum value for coatings deposited at 10 Hz frequency and 10% duty cycle.

1.4.1.5 Ni-WC Composite Coatings

WC is one of the hard metals widely used in tribological applications. Surender *et al.* analyzed wear characterization of Ni-WC composite coatings [49]. Microhardness of composite coatings significantly increased with increasing WC content in the composites due to dispersion strengthening effect. Coefficient of friction of these composite coatings decreased with increasing amount of WC as does the hardness of composite coatings.

This reduction in coefficient of friction was mainly based on fundamental friction principle. The worn surfaces have undergone hertzian contact damage with elastic flattering of protruding WC particles [49].

M. Surrender *et al.* studied electrochemical behavior of Ni-WC composite coatings [50]. WC reinforcements in nickel composite coatings significantly affects the stability of passive film and causes a positive shift in passivation potential, reduction in passive range and higher passive current densities compared to pure nickel coatings.

1.4.1.6 Ni-CNT Composite Coatings

Due to excellent mechanical properties such as high strength, high elastic modulus, and large elastic as well as fracture strain, carbon nanotubes (CNTs) are attracting significant interest as reinforcement in metallic coatings. CNTs have significant interests as reinforcement in various metallic, ceramic, and polymeric materials to impart strength, toughness, and wear/corrosion resistance. [43, 51, 52]

Arai *et al.* analyzed tribological performance of Ni-CNT composite coatings [53]. The coefficient of friction of Ni-CNT composite coatings significantly reduced due to intrinsic self lubricity of CNTs. Chen *et al.* studied corrosion behavior of Ni-CNT composite coatings[51]. Incorporation of CNTs into nickel matrix significantly increased corrosion resistance as the reinforced CNTs act as physical barriers to corrosion process by filling in crevices, gaps, and micron holes on the surface of nickel coatings. Uniform dispersion of CNTs in composite coatings was restricting localized corrosion and

corrosion potential of composite coatings increases towards positive values which promotes homogeneous corrosion.

Arai *et al.* fabricated Ni-CNT composite coatings with excellent thermal conductivity by electrodeposition[54]. Improvement in thermal conductivity of pure nickel coatings would be useful in electronic devices because of heat dissipation problem. Ni-CNT composite coatings attained thermal conductivity of 109 Wm^{-1} k^{-1} which is almost twice that of pure nickel coatings.

1.4.2 Properties of Nickel Composite Coatings

Mechanical properties of Nanocrystalline materials mainly depend on microstructure of material enables dislocation theory correlating with strength and ductility of these materials. Nickel composite coatings consist of nickel matrix containing dispersion of second phase particles, such as Al_2O_3, Si_3N_4, SiC, Cr_2O_3, WC, diamond, PTFE, graphite, or even liquid containing microcapsules to improve mechanical, tribological, and corrosion resistance properties of nano-composites. These second phase particles act as physical barrier to dislocation movement and grain boundary sliding resulting into significant improvement in mechanical properties of composite coatings.

1.4.2.1 Hardness

Hardness of material is defined as the resistance of a material to deformation particularly permanent deformation, indentation or scratching [55, 56]. Generally, hardness is related

to the tensile yield stress due to geometrical constraint resulting from deformation by [44, 57, 58]

$$H = 3\sigma_y \quad (1)$$

Addition of ceramic particles to synthesize composite coatings act as a barrier to dislocation movement and grain boundary sliding thus increasing hardness of composite coatings. Increase in hardness of composite coatings is due to the combined effect of grain refinement due to Hall-Petch mechanism and uniform dispersion of nano-particles due to Orowan mechanism. Therefore, effect of reinforced particles in composite coatings on hardness depends mainly on volume content as well as size and distribution of these particles in the metal matrix [47]. Hardness of composite coatings mainly influenced by two aspects:

(a) Hardness of metal matrix which is determined by microstructure of coatings.

(b) Volume content of reinforced particles in the composite coatings.

A comparison of Vickers microhardness for a wide range of nickel composite coatings is shown in Fig. 1.7. It clearly shows significant improvement in hardness of composite coatings compared to pure nickel coatings.

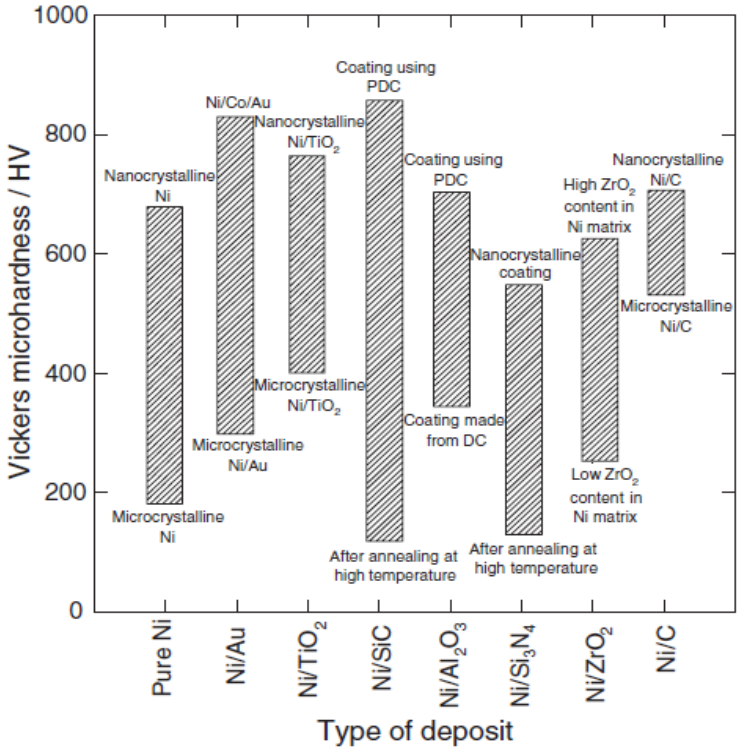

Fig. 1.7 *Vickers microhardness values for different ranges of particle size in nickel deposit. The values are displayed from minimum to maximum (bottom to top) found in the literature. DC: direct current; PDC pulsed direct current [17].*

1.4.2.2 Corrosion Resistance

Nickel composite coatings have better corrosion resistance than pure nickel coatings because reinforced second phase particles disturb the regular growth of nickel crystal and promote new nucleation site. This makes structure of composite coatings more finely crystalline and hence improved corrosion resistance of composite coatings [59, 60]. Addition of these particles in composite coatings will decrease corrosion current density and will shift corrosion potential of composite coatings towards more noble direction i.e.

positive value. Amadeh *et al.* performed electrochemical experiments to analyze corrosion behavior of (Ni-SiC) composite coatings [60].

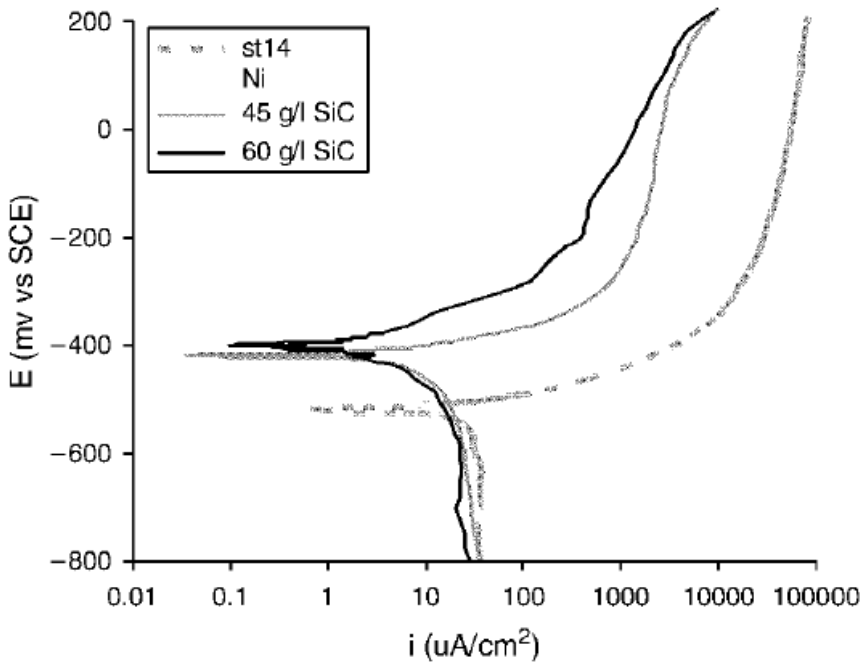

Fig. 1.8 *Polarization curves of st14 steel, pure nickel and composite coatings produced at the current density of 4 A/dm^2, d.c.= 30%, Frquency= 10Hz from baths containing 45 g/L and 60 g/L SiC [60].*

Fig. 1.8 clearly shows that the corrosion resistance of composite coatings has significantly improved compared to pure nickel coatings and stainless steel substrate [60]. Cathodic polarization curves for pure nickel and Ni-SiC composite coatings shown in Fig. 1.9. Addition of SiC particles act as obstacles to the initiation and development of defect corrosion and also filled in crevice, gaps, and micron holes of nickel matrix

resulting in significant improvement of corrosion resistance of composite coatings [46]. Almost all nickel composite coatings reinforced with Al_2O_3 [59, 61] SiC [46, 60, 62] , TiO_2 [34], CNTs [51, 63, 64], Si_3N_4 [65], and WC [50] show better corrosion resistance compared to pure nickel coatings.

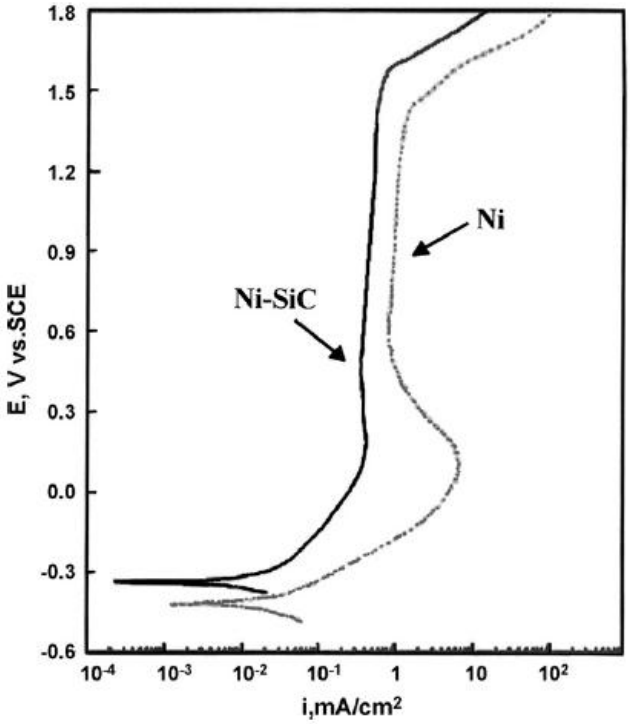

Fig. 1.9 *Cathodic polarization curves of nickel and Ni–SiC nano-composite coating (containing 3% SiC) in 0.5 M NaCl solution [60].*

1.4.2.3 Wear Resistance

Nickel composite coatings reinforced with Al_2O_3 [9, 14, 45], WC [49], TiO_2 [34], ZrO_2 [47], CNTs [53, 66-68], SiC [22, 46, 69, 70], and Si_3N_4 [70] show better wear resistance compared to pure nickel coatings. The improvement in microhardness as well as wear resistance of composite coatings mainly depends on reinforced second phase particles in

the nickel matrix act as a physical barrier to nickel grain growth and plastic deformation of nickel matrix under loading promotes grain refining and dispersive strengthening effect to improve microhardness as well as wear resistance composite coatings [46]. Vaezi *et al.* characterized tribological behavior of (Ni-SiC) composite coatings and compared with pure nickel coatings [46]. Fig. 1.10 shows that composite coating showed less wear rate than pure nickel coatings. The increase in microhardness and decrease in the wear rate of composite coatings is due to combination of grain refining and dispersion strengthening effect. These effects become stronger with increasing SiC content, thus microhardness and wear resistance of composite coatings increases with increasing SiC content in the coatings.

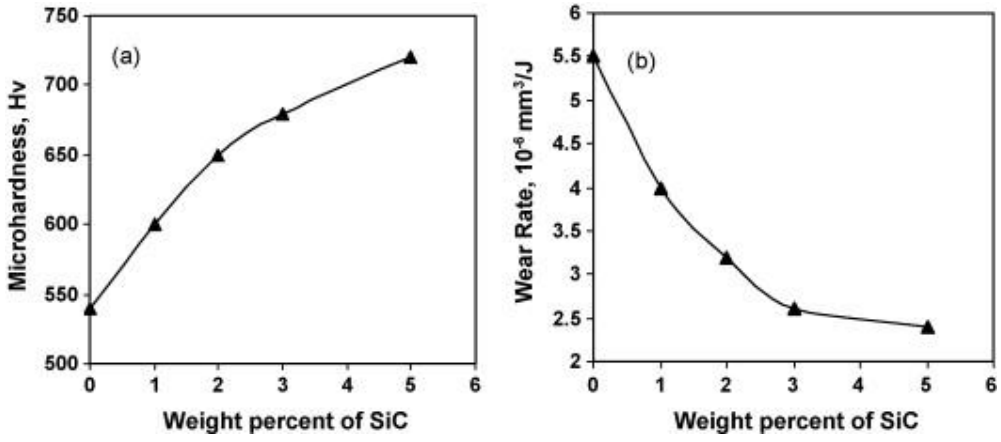

Fig. 1.10 *Microhardness (a) and wear rate (b) of the Ni–SiC nano-composite coating vs. weight percent of SiC nano-particulates [46].*

Arai *et al.* employed CNTs as reinforcement for synthesizing composite coatings [53]. They showed the superior solid lubrication of Ni-CNTs composite film is schematically illustrated in Fig. 1.11

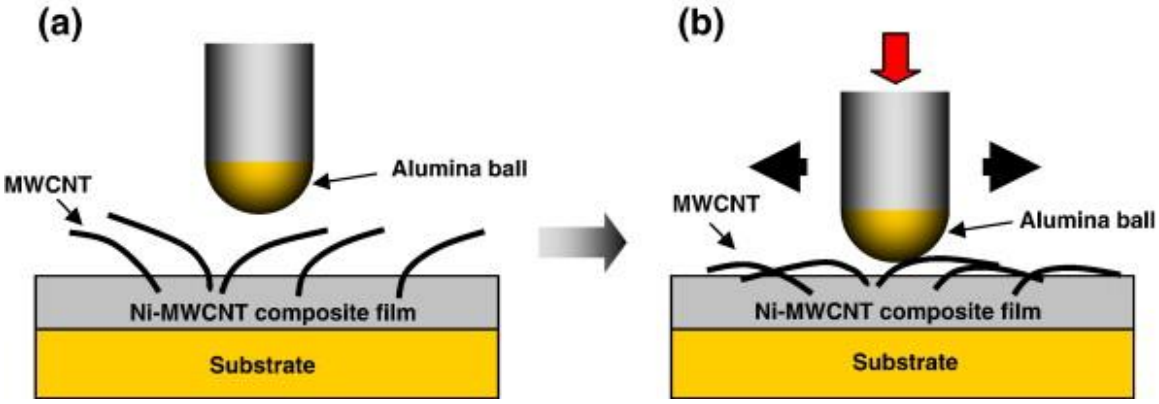

Fig. 1.11 *A schematic illustration of the superior solid lubrication of a Ni–MWCNT composite film: (a) before the wear test and (b) during the wear test [53].*

Initially CNTs are arranged vertically with respect to alumina ball (i.e. counter body) resulting in higher coefficient of friction. Once wear test starts, alumina ball scratches composite film and surface is physically deformed. Consequently, CNTs are gradually arranged transversely resulting in lowering the coefficient of friction and further improving wear resistance of composite coatings. Nickel composite films with Al_2O_3 reinforcement show better wear resistance compared to pure nickel coatings due to combined effect of hard nature of reinforced particles and strengthening effect caused by incorporation of Al_2O_3 particles [45].

During wear tests of composite coatings, friction, and wear are mainly determined by distribution and properties of reinforced particles. Uniform distribution of reinforced

particles in the composite coatings improves hardness due to dispersion hardening effect. The coefficient of friction of composite decreases with increase in volume content of reinforced particles as well as hardness of composite coatings. This decrease in coefficient of friction is due to matrix hardening and elastic interaction of counter body with reinforced particles. This follows from following fundamental relationship between friction and material properties.

$$\mu = \tau_a / E * (\sigma_p / R_p) \quad \text{Elastic contact} \quad (2)$$

$$\mu = \tau_a / H \quad \text{Plastic contact} \quad (3)$$

Where, μ is the coefficient of friction, E^* is the composite or effective modulus, σ_p and R_p are the composite standard deviation in the asperity height distribution and composite radius of summits, τ_a is the average shear strength of dry contact and H is the hardness. Tribological behavior in most of composite coatings will be more like an elasto-plastic contact, with nickel matrix undergoing plastic deformation whereas severe interaction with reinforced particles being of elastic nature [49].

1.4.3 Applications of Nickel composite coatings

- **Ni-Al_2O_3 composite coatings**

These composite coatings are widely used in applications which require abrasion and heat resistant coatings, corrosion resistant coatings, self lubrication films and thermally graded structures [44, 59]. Nickel composite coatings prove to be a good alternative for chromium coatings. Ni-alumina composite coatings finds application for coatings of

engine cylinders, high pressure valves, and dies, in the production of musical instruments, drill fitting, car accessories, small aircraft, and electrotechnical parts [59]. One of the most promising applications for these composite coatings is in micro devices [13, 23, 71].

- **Ni-SiC composite coatings**

Ni- SiC composite coatings are widely used for the protection of friction parts due to their excellent wear resistance and low cost [15, 22, 46, 69]. Also, these coatings find applications in combustion engine and casting moulds due to their anti-wear property [46].

- **Ni-CNT composite coatings**

Recently carbon nanotubes (CNTs) have attracted significant interests as reinforcements in various metallic, ceramic, and polymeric materials to impart strength, toughness, and wear/corrosion resistance [43, 51, 52, 72]. The CNT reinforcement in metallic materials is particularly attractive for structural applications where high specific strength/wear resistance is desired and for functional applications where excellent thermal/electrical properties are important [73-75]. These composite coatings find applications in nano devices such as nano diodes, nano transistors due to novel electronic properties of CNTs [51, 67]. Due to excellent anti-wear property of Ni-CNT composite coatings can be find application in the aerospace, automobile, and other industries as frictional components [53].

1.5 Objective

1.5.1 Effect of Plating Conditions (DC, PC, PRC) on Microstructure and Properties of Pure Nickel and Nickel Composite Coatings (Ni, Ni-Al_2O_3, Ni-SiC, and Ni-ZrO_2)

Pulse current (PC) and pulse reverse current (PRC) electrodeposition techniques bring new era in the electrodeposition of metals, alloys, and metal matrix composites. Compared with conventional direct current (DC) electrodeposition, PC and PRC electrodeposition offers more control over the process parameters which can also be adjusted independently. Metal coatings fabricated by PC and PRC electrodeposition techniques exhibit unique microstructure and compositions than those obtained by DC electrodeposition [47]. Recently PC and PRC electrodeposition techniques widely used in fabricating composite coatings. PRC composite coatings showed uniform dispersion of alumina particles as well as improvement in alumina reinforcement in the coatings compared to DC composite coatings [76, 77]. Nickel composite coatings (Ni-Al_2O_3, Ni-SiC, and Ni-ZrO_2) are fabricated by DC, PC, and PRC electrodeposition techniques to optimize the electrodeposition method for further work. Pure nickel coatings are also fabricated by DC, PC, and PRC electrodeposition techniques with same electrodeposition parameters for comparison.

1.5.2 Effect of Reinforcement Content on Microstructure and Properties of Ni-Al_2O_3 Composite Coatings

Ni-Al_2O_3 composite coatings are fabricated by varying alumina concentration in the electroplating bath. Ni-Al_2O_3 composite coatings offered higher hardness, wear, and

corrosion resistance due to high hardness of Al_2O_3 (2000-2300 HV) and corrosion resistant nickel metal [25]. Nickel composite coatings are mainly used to increase the abrasion resistance of metal surface in microdevices. The properties of nickel composite coatings mainly depend on size, distribution, and concentration of alumina particles in nickel matrix. Higher concentration and uniform dispersion of second phase particles in the metal matrix enhance corrosion and wear resistance of composite coatings. Research has been carried out on the effect of pulse parameters on the mechanical and tribological properties of nano-composite coatings [9, 30, 46, 59]; but very few examined the influence of alumina concentration on microstructure, mechanical, and tribological properties of composite coatings. Pulse electrodeposition technique not only significantly improves the hardness, wear, and corrosion resistance, but also decreases porosity as well as internal stresses in the composite coatings [30]. In this work, effect of alumina concentration on microstructure, mechanical, and tribological properties of nickel composite coatings is examined.

1.5.3 Pulse Electrodeposition of Ni-CNT Composite Coatings

The processes such as hot pressing [78], hot extrusion [79, 80], rapid solidification [81], sintering [82], and plasma spray forming technique [83] have been extensively employed for fabricating CNT reinforced metal matrix composites. Significant improvement in mechanical properties of composites obtained by plasma spray forming and sintering has been reported [82, 83]. The composites obtained by rapid solidification techniques showed significant improvement in thermal and electrical properties but reduction in

saturation magnetic moments [81]. Some reports on fabrication of metal matrix composites using hot pressing and hot extrusion reported insignificant improvement in mechanical and electrical properties of composites primarily due to inhomogeneous dispersion of CNTs into the metal matrix [78-80]. Also, the fabrication of CNT reinforced metal matrix composites by these processes is often associated with appearance of porosity in the composite and complex interfacial reactions between CNTs and matrix material [83, 84]. While some progress has been made in the fabrication of bulk CNT reinforced metal matrix composites using conventional forming and powder metallurgical methods, very few reports are published on synthesis of CNT reinforced metal matrix composite coatings [85, 86].

Nickel is widely used in electronic devices such as circuit boards and switches due to its good corrosion resistance and low diffusion coefficient but it has poor thermal conductivity [54]. Heat dissipation is a common problem in almost all electronic devices therefore materials with excellent thermal conductivity are required. The CNT reinforced nickel composite coatings are expected to exhibit excellent thermal conductivity and mechanical properties as compared to pure nickel coating. In the present investigation we explore the possibility of reinforcing CNTs in nickel coating using pulse electrodeposition technique. While the basic pulse electrodeposition set-up for reinforcing CNTs in nickel matrix is similar to that of reinforcing particulate (Al_2O_3, ZrO_2, and SiC), uniform dispersion of CNTs throughout the nickel metal matrix is important to improve the mechanical as well as electrical properties of Ni-CNT composites. The present work mainly analyzes the effect of reinforcement of CNTs on the evolution of phases, surface morphology, crystallographic texture, mechanical

properties such as microhardness and tribological properties such as wear resistance of the composite coating. In order to evaluate effect of reinforcement of CNTs in the coating, pulse electrodeposition was also performed to deposite pure nickel coatings using same pulse parameters.

CHAPTER 2

EXPERIMENTAL DETAILS

2.1 Watts Bath

Two types of electroplating bath commonly used for electrodeposition of nickel are Watts bath and sulphamate bath. Standard Watts solution consists of $NiSO_4.6H_2O$ (Nickel sulphate hexahydrate), $NiCl_2.6H_2O$ (Nickel chloride hexahydrate), and H_3BO_3 (Boric acid). Table 2.1 shows content of these chemicals for making of 1 L. of electroplating bath.

Table 2.1 Overview of the composition of chemicals for Watts bath

Bath composition	
Electrolyte (Watts bath)	
$NiSO_4.6H_2O$	265 g/L
$NiCl_2.6H_2O$	48g/L
H_3BO_3	31g/L

Boric acid is added to lots of nickel plating baths. Boric acid acts as buffer to control the pH in the cathode solution interface [87], also acts as catalyst which lowers the overvoltage for Ni deposition as well as considered as a homogeneous catalyst for Ni deposition in the Watts bath. pH of the electroplating bath is adjusted to 4.0 by addition of NaOH (Sodium Hydroxide) to the electroplating bath.

2.2 Pulse Generator

A pulse power supply equipment (model 20-10-30) manufactured by Dynatronix is shown in *Fig. 2.1*. The displays on the left side shows current and voltage respectively whereas right hand side display shows all the set values for a particular experiment (i.e. current density, duty cycle, frequency, and duration of the experiment). Pulse generator has a capacity of producing 20 V voltages and 30 Amp peak current. Maximum frequency of 10,000 Hz can be attained by this pulse generator. Schematic and actual experimental setups of electrodeposition process are shown in *Fig. 2.2* and *Fig. 2.3*.

Fig. 2.1 *Pulse Generator used for electrodeposition process*

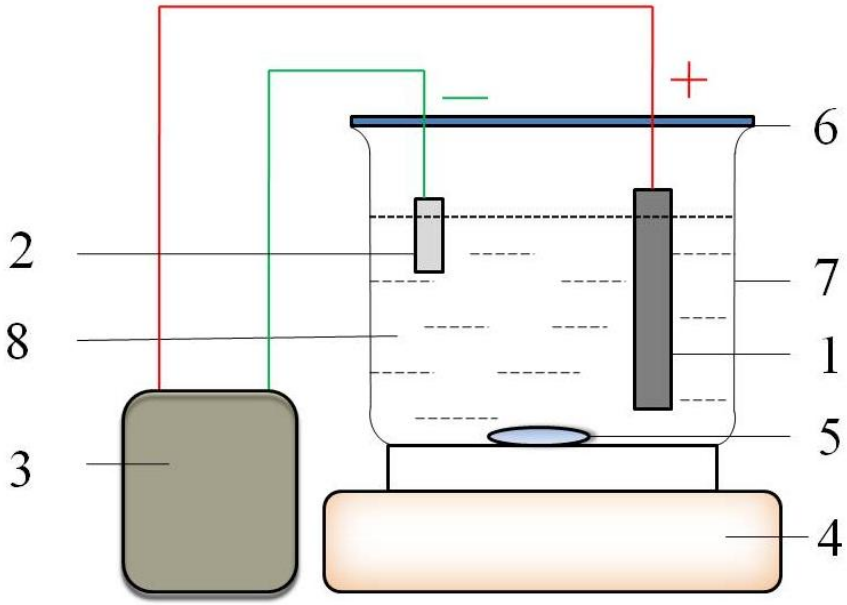

Fig. 2.2 *Schematic diagram of the pulse-electrodeposition system: 1. Nickel plate, 2. Stainless steel plate, 3. Pulse generator, 4. Hot plate stirrer, 5. Stirring bar, 6. Locating plate, 7. Beaker, and 8. Electrolyte.*

Fig. 2.3 *Actual Experimental setup for electrodeposition process*

2.3 Processing of Nickel Composite Coatings

2.3.1 Effect of Plating Conditions (DC, PC, PRC) on Microstructure and Properties of Pure Nickel and Nickel Composite Coatings (Ni, Ni-Al_2O_3, Ni-SiC, and Ni-ZrO_2)

The nickel composite coatings (Ni-Al_2O_3, Ni-SiC, and Ni-ZrO_2) prepared by electrodeposition from Watts solution suspended with nanoparticles. The nanoparticles used as reinforcement have (Al_2O_3=150 nm, ZrO_2= 30-60 nm, SiC=200 nm) particle sizes. Before electrodeposition electrolyte was stirred for about 24 hours using magnetic stirrer. All the electrodeposition experiments were carried out at room temperature. A stainless steel plate (with an area of 8 cm^2) and pure nickel plate (with an area of 100 cm^2) were used as cathode and anode respectively. DC, PC, and PRC electrodeposition techniques were used to fabricate the coatings and corresponding parameters are given in the Table 2.2.

For comparison, pure nickel coatings were prepared in same electroplating bath without nanoparticles under same electrodeposition conditions. After electrodeposition of 60 min., the coatings were washed and cleaned using deionized water in ultrasonic cleaner.

Table 2.2 Electrodeposition parameters for synthesizing nickel composite coatings

Electrodeposition parameters	
Direct Current (DC) Electrodeposition	
Current density	3 A/dm^2
Plating time	60 min
Electrolyte agitation (Magnetic stirring)	200 rpm
Pulse Current (PC) Electrodeposition	
Peak current density	3 A/dm^2
Plating time	60 min
Electrolyte agitation (Magnetic stirring)	200 rpm
Duty Cycle	20%
Frequency	10 Hz
Pulse Reverse Current (PRC) Electrodeposition	
Forward Peak current density	3.3 A/dm^2
Electrolyte agitation (Magnetic stirring)	200 rpm
Forward Duty Cycle	10%
Forward Frequency	1000 Hz
Forward duration	200 ms
Reverse Peak current density	3 A/dm^2
Reverse Duty Cycle	20%
Forward Frequency	1000 Hz
Reverse duration	50 ms
Plating time	60 min
Anode	Nickel
Cathode	Stainless steel

2.3.2 Effect of Reinforcement Content on Microstructure and Properties of Ni-Al_2O_3 Composite Coatings

The electroplating bath for synthesizing Ni-Al_2O_3 composite coatings was a Watts solution with addition of alumina powder varying from 0 g to 40 g/L. The electroplating parameters are given in Table 2.3.

Table 2.3 Overview of the pulse-electrodeposition parameters for preparation of pure Ni and Ni-Al_2O_3 composite coatings

Pulse Current (PC) Electrodeposition parameters	
Peak current density	3 A/dm^2
Plating time	8 hrs.
Electrolyte agitation (Magnetic stirring)	200 rpm
Duty Cycle	20%
Frequency	10 Hz

Different amounts of alumina loading were used in the experiments to investigate its influence on the microstructure, mechanical, and tribological behavior of nickel composite coatings. Each electroplating bath was agitated by magnetic stirrer for 24 hrs prior to electrodeposition and also during plating. A stainless steel plate (with an area of 8 cm^2) and pure nickel plate (with an area of 100 cm^2) were used as cathode and anode respectively. After electrodeposition for 8 hrs. coatings were washed and cleaned using

deionized water in ultrasonic cleaner.

2.3.3 Pulse electrodeposition of Ni-CNT composite coatings

2.3.3.1 Pretreatment of Multi-walled Carbon Nanotubes:

The CNTs are quasi one-dimensional nanomaterials mostly available in bundled form because of strong Vander Waals interactions between the tube walls [88]. One of the major issues with the fabrication of CNT reinforced composite coatings is related to the non-uniform dispersion of CNTs in the composite matrices. In this investigation, surface treatment of CNTs was carried out using nitric acid to improve the dispersion of the CNTs into the electrodeposited Ni-CNT coating. The nitric acid surface treatments form carboxylic acid groups on CNTs and help in uniform dispersion of CNTs without any additional dispersing additive [89, 90]. In the present investigation, 1 g CNTs were added into 1000 ml of 8M nitric acid (HNO_3) in a glass bottle. The mixture was subsequently sonicated in an ultrasonic bath at 40-50° C for about 1.5 hrs. The mixture was diluted with 2000 ml deionized water and then vacuum filtered using a 0.2 µm Polytetrafluoroethylene (PTFE) filter. The obtained solid mixture was washed with deionized water on the filter until the filtrate was neutral. The filtrate was neutral at pH 7 which was checked with a pH meter. After this, the obtained CNTs were dispersed in the electrolyte without any addition of dispersing agent.

2.3.3.2 Fabrication Ni and Ni-CNT Composite Coatings:

Two types of coatings deposited on stainless steel substrate using pulse electrodeposition are pure nickel coating and Ni-CNT composite coating with nitric acid pretreatment of CNTs. The plating bath for pulsed electrodeposition of Ni-CNT composite coating was standard Watts solution. The plating parameters for depositing pure nickel coating are given in Table 2.4. For Ni-CNT composite coatings, 1 g of multiwalled CNTs (pretreated with nitric acid) were mixed in 1 L. basic electrolyte. The CNTs used have outside diameter of 30-50 nm, inside diameter of 5-15 nm, and length of 10-20 μm. Before pulse electrodeposition, the plating bath was sonicated in ultrasonic cleaner for about 1 hour at room temperature followed by stirring for 5 hours. A stainless steel plate (with an area of 2 cm^2) and a pure nickel plate (with an area of 20 cm^2) were used as cathode and anode respectively.

Table 2.4 Overview of the pulse-electrodeposition parameters for preparation of pure Ni and Ni-CNTs composite coatings

Pulse Current (PC) Electrodeposition parameters	
Peak current density	5 A/dm^2
Plating time	60 min
Electrolyte agitation (Magnetic stirring)	200 rpm
Duty Cycle	20%
Frequency	10 Hz

The stainless steel substrates were mechanically polished using a sequence of 400, 600, and 1200 mesh emery papers followed by a sequence of cleanings (acetone, ethanol, de-ionized water) to prepare the substrate surface for electrodeposition. The stainless steel substrate was then activated in 25% sulfuric acid (H_2SO_4) solution for about 10 minutes. This activated stainless steel substrate was placed parallel at a distance of 5 cm from the vertically oriented nickel plate in the above plating bath. During the electrodeposition process, the plating bath was slowly stirred with the help of a hot plate stirrer in order to prevent agglomeration of CNTs in the electrolyte suspension. Also, the electrolyte temperature was maintained at 25° C with the help of a hot plate stirrer. The electrodeposition was carried out with duty cycle of 20% and pulse frequency of 10 Hz. The current density of 5 A/dm^2 was maintained throughout the electrodeposition process by keeping T_{ON} time equal to 20 ms and T_{OFF} time equal to 80 ms. The pulse parameters used in the present investigation are found to give adherent Ni-CNT composite coatings. Similar regimes of pulse parameters are also reported in the literature on pulse electrodeposition of nanocomposite coatings [9, 30]. After electrodeposition for 30 min, the composite coating was washed and cleaned in deionized water.

2.4 Material Characterization

2.4.1 Phase and Micro Structural Analysis

The phase analysis of composite coatings was conducted using Phillips Norelco X-Ray Diffractometer operating with CuKα (λ= 1.54178 Å) radiation at 45 kV and 40 mA. The diffraction angle (2θ) was varied between 30º and 80º 2θ at a step increment of 0.02º with a count time of 1 s. Crystallite size of nickel was calculated for pure nickel and Ni-composite coatings using Scherrer's equation, given by [91]:

$$FWHM = \frac{K\,\lambda}{D\cos\theta}\,\frac{180^\circ}{\pi}, \tag{4}$$

Where *FWHM* = Full width half maxima in 2θ degrees; *D*= crystallite size in nm; *K*= constant (usually evaluated as 0.94); and *λ* = wavelength of Cu Kα radiation (0.154 nm).

To quantify the crystallographic textures of nickel associated with nickel and nickel composite coatings, texture coefficients (TC) for predominant (h k l) peaks in XRD patterns were calculated. The texture coefficient (TC) for each (h k l) reflection is given by [92]:

$$\mathrm{TC}(h\ k\ l) = \frac{I(h\ k\ l)}{I_0(h\ k\ l)}\left\{\frac{1}{n}\sum\frac{I(h\ k\ l)}{I_0(h\ k\ l)}\right\}^{-1}, \tag{5}$$

where *I(h k l)* are measured intensities of (*h k l*) reflection, $I_0(h\ k\ l)$ are powder diffraction intensities of nickel and *n* is the number of reflections used in the calculations.

The surface morphology of coatings was observed using Scanning Electron Microscope (JSM-6360, JEOL) and weight percentage of co-deposited nanoparticles was evaluated by energy dispersive spectroscopy (EDS). FEI Quanta 600 field-emission gun

Environmental Scanning Electron Microscope with an Evex EDS X-ray microanalysis system and HKL EBSD system is used for EDS analysis.

2.4.2 Raman Spectroscopy

Presence of CNTs in the composite coatings is very difficult to determine using XRD or EDS analysis. Raman spectroscopy is an efficient technique used to determine presence of CNTs in the coatings. Raman spectra were acquired using ramascope 2000 (Renishaw, UK). Raman microspectrometer. The scattered light from Ar^{+} laser (excitation wavelength 51435 nm) was dispersed with diffraction grating and detected with charge coupled device.

2.4.3 Surface Roughness

Surface roughness of composite coatings were measured using (Perthometer Mahr^{TM}, Province, RI) model M1 having measuring range up to 150 µm. Tracing length used for measurements was 5.6 mm.

2.5 Mechanical Testing

2.5.1 Microhardness Testing

A microhardness tester (Buehler^{TM}) was used for measuring hardness of coatings by performing Vickers indentation at a loading force of 25 g and holding time of 10 seconds.

The final value quoted for the hardness of the coatings was the average of 10 measurements.

2.5.2 Wear Test

The wear tests were performed on ball-on-disc tribometer (Nanovea^{TM}, Irvine, CA) at room temperature without any lubrication. An alumina ball (diameter 6 mm) was used as counter body to create wear track of 4 mm in diameter on the sample surface. The wear tests were performed by using load of 7 N and velocity of 150 rpm for equal intervals of 4 minutes. The position of specimen on the tribometer was maintained after each weight-loss reading such that wear continues on the same worn track during consecutive wear testing.

CHAPTER 3

RESULTS AND DISCUSSION

3.1 Effect of Plating Conditions (DC, PC, PRC) on Microstructure and Properties of Pure Nickel and Nickel Composite Coatings (Ni, Ni-Al_2O_3, Ni-SiC, and Ni-ZrO_2)

3.1.1 Coating Surface Morphology:

SEM micrographs showing surface morphologies of DC, PC, and PRC electrodeposited pure nickel (Ni) and nickel composite (Ni-Al_2O_3, Ni-SiC, and Ni-ZrO_2) coatings are presented in Fig. 3.1. Also, the variation of surface roughness parameters (R_a and R_z) with plating conditions for these coatings is shown in Fig. 3.2. The Ni coatings fabricated using PC and PRC technique exhibited better uniformity and finer grain structure compared to the coatings obtained by DC deposition techniques. High instantaneous current density during PC and PRC deposition seems to promote the nucleation of the grains on the surface resulting in finer grain structure in the Ni coating. The PRC deposited Ni coatings exhibited lowest surface roughness values (Ra<50 nm; Rz~0.3 μm). The surface roughness values for the DC deposited Ni coatings were highest (Ra~75 nm; Rz~0.5 μm). All the nickel composite coatings (Ni-Al_2O_3, Ni-SiC, and Ni-ZrO_2) exhibited higher surface roughness compared to pure nickel coatings. For the nickel composite coatings, the PC plating condition resulted in more compact, uniform, and

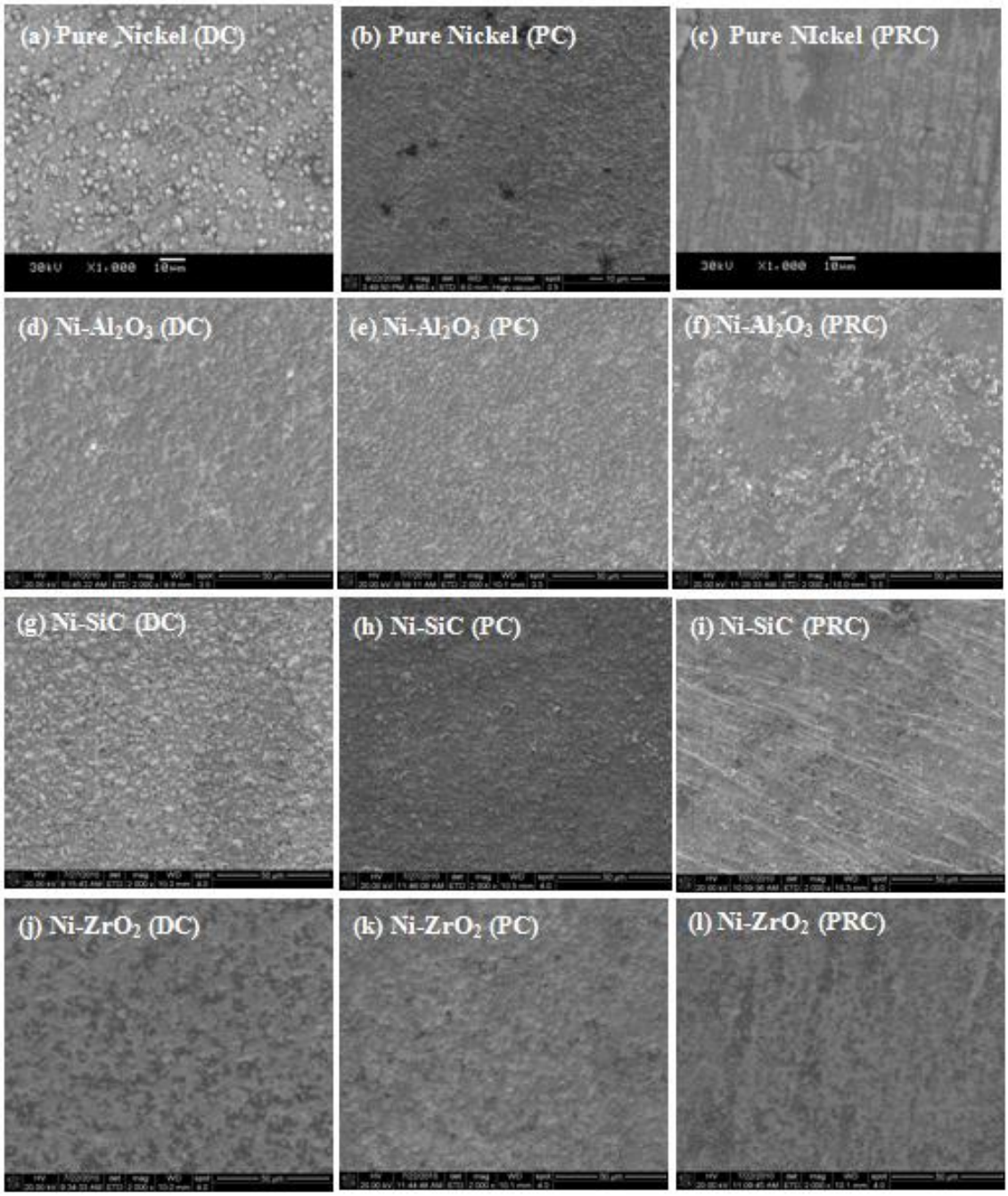

Fig. 3.1 *Surface micrographs from (a-c) pure nickel, (d-f) Ni-Al_2O_3, (g-i) Ni-SiC, and (j-l) Ni-ZrO_2 coatings are deposited by DC, PC, and PRC electrodeposition methods.*

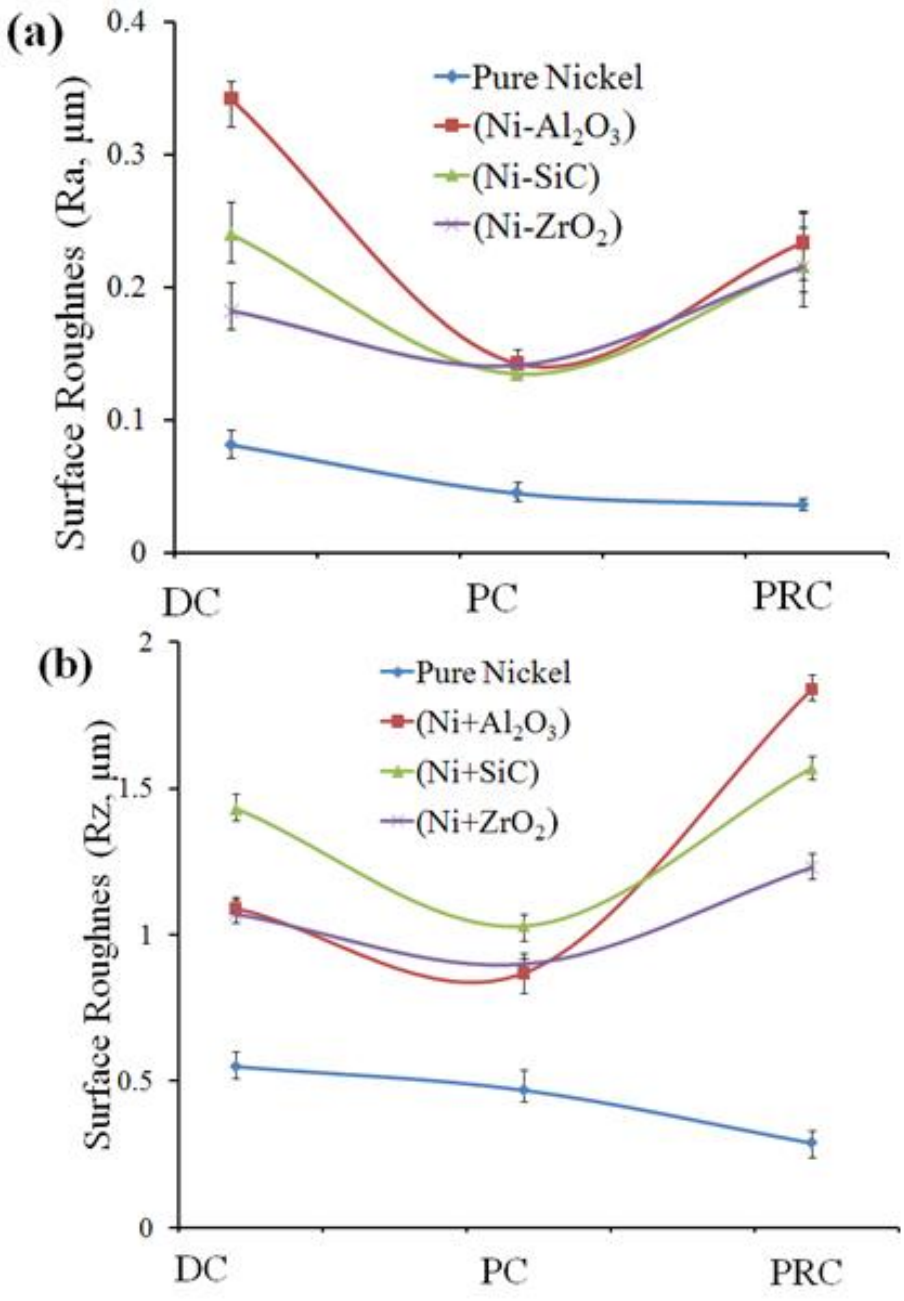

Fig. 3.2 *Surface roughness of nickel and nickel composite coatings deposited by DC, PC, and PRC electrodeposition methods: (a) Ra, and (b) Rz.*

finer microstructure of the coatings. The values of surface roughness parameters for these PC codeposited composite coating were minimum (Ra~120-150 nm; Rz~0.9-1.1 μm). The surface microstructures of the DC codeposited composite coatings show coarser granular features resulting in highest surface roughness values for these coatings. The surface microstructure of the PRC codeposited composite coatings show surface inhomogeneities due to agglomeration of the reinforcement particles of the surface. This also resulted in higher values of surface roughness parameter for PRC codeposited composite coatings.

3.1.2 Coating Composition:

The variation of weight percentage of reinforced nanoparticles in the nickel composite coating as a function of co-deposition conditions (DC, PC, and PRC) is shown in Fig. 3.3. For all the composite coatings (Ni-Al_2O_3, Ni-SiC, and Ni-ZrO_2), the figure clearly indicates significantly increased reinforcement content in the coating prepared by PC and PRC co-deposition. The reinforcement content is minimum in the coatings deposited using DC co-deposition. As mentioned earlier, the periodic alternation of current (between positive and zero values for PC, and between positive and negative values for PRC) discharges the electric double layer formed around the cathode, and thereby allowing better penetration of nanoparticles (with adsorbed ions on the surface) towards cathode. The adsorbed ions on the surface of the nanoparticles subsequently get reduced at the cathode causing entrapment (reinforcement) of the nanoparticles in the growing coating. Also, for the similar codeposition conditions (DC, PC, or PRC), the

reinforcement content of alumina in the Ni-Al_2O_3 composite coating is greater than zirconia in the Ni-ZrO_2 and silicon carbide in the Ni-SiC composite coatings. While exact mechanism for this observation is not yet known, this seems to be due to distinctly different size/density of the nanoparticles and their interactions with the ions in the electrolyte.

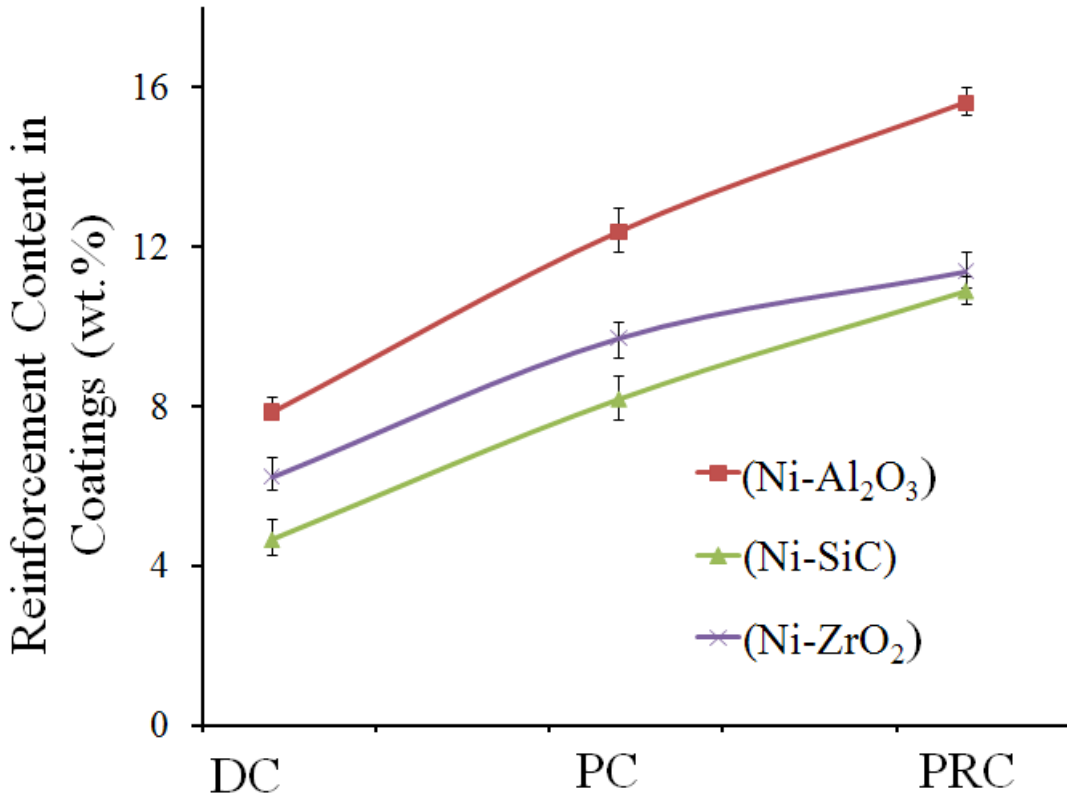

Fig. 3.3 *Variation of wt.% of nanoparticles in nickel composite coatings deposited by DC, PC, and PRC electrodeposition methods.*

3.1.3 Crystallite Size and Crystallographic Texture:

The x-ray diffraction (XRD) patterns for pure nickel and nickel composite (Ni-Al_2O_3, Ni-SiC, and Ni-ZrO_2) coatings deposited by DC, PC, and PRC plating conditions are presented in Fig. 3.4. All the XRD patterns show typical peaks corresponding to (111) and (200) crystallographic planes of nickel. Note that the peaks corresponding to reinforced nanoparticles (i.e. Al_2O_3, SiC, and ZrO_2) could not be resolved in XRD patterns from composite coatings due to very low reinforcement content. To understand the influence of electrodeposition condition (DC, PC, and PRC) on the development of coating microstructure and microtexture, detailed analysis of XRD patterns was conducted.

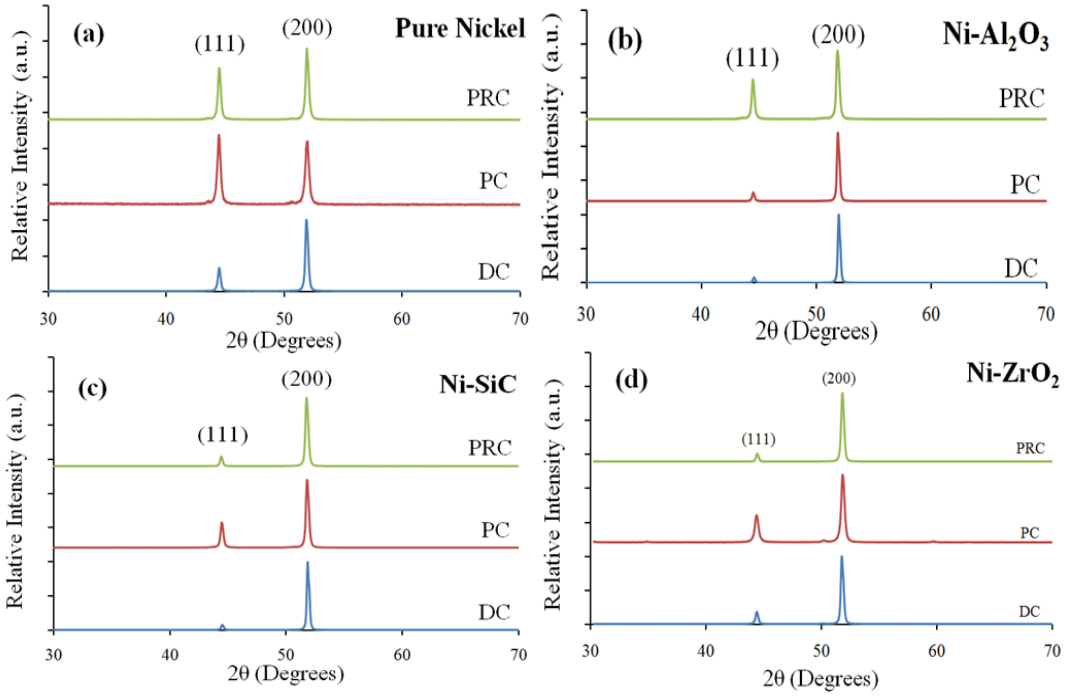

Fig. 3.4 *X-ray diffraction patterns from (a) pure nickel, (b) Ni-Al_2O_3, (c) Ni-SiC, and (d) Ni-ZrO_2 composite coatings deposited by DC, PC, and PRC electrodeposition methods*

Table 3.1 shows crystallite sizes for all the nickel and nickel composite coatings calculated using FWHM of prominent (111) reflection in Scherrer equation. For all the coatings, crystallite size of the nickel matrix is less than 50 nm.

Table 3.1 Crystallite size for pure nickel and nickel composite coatings.

Coatings	**Crystallite Size (nm)**		
	DC	**PC**	**PRC**
Pure Nickel	46	37	42
Ni-Al_2O_3	37	30	34
Ni-SiC	37	32	35
Ni-ZrO_2	35	28	34

For all the coatings deposited using DC electrodeposition, the intensity of (200) peaks is highest indicating preferred orientation of (200) plane parallel to coating surface. Apparently, [100] is the preferred grain growth direction for face centered cubic crystals. Note that (111) peak at $2\theta=44.508°$ is the strongest peak (relative intensity=100%) in the standard XRD pattern from randomly oriented polycrystalline nickel (JCPDS: 04-0850). As indicated in the figure, the intensity of (111) peaks in the XRD patterns of pure nickel and nickel composite coatings increased for PC and PRC deposition indicating more random crystallographic texture in these coatings (approaching that in standard XRD pattern from randomly oriented polycrystalline nickel). The atomic density of (111) plane is higher than that of (200) plane in FCC crystal structure of nickel, so surface energy of (111) plane is lower than that of (200) plane. It seems that nickel atoms migrate from

Table 3.2 Texture coefficients (TCs) of various (*hkl*) planes for standard sample, pure nickel, and nickel composite coatings.

Coatings	Texture Coefficient (TC)	
	(111)	**(200)**
Standard Sample	1	1
Pure Nickel		
DC	0.24	1.76
PC	0.64	1.36
PRC	0.47	1.53
Ni-Al_2O_3		
DC	0.06	1.93
PC	0.10	1.90
PRC	0.39	1.61
Ni-SiC		
DC	0.06	1.94
PC	0.27	1.73
PRC	0.11	1.89
Ni-ZrO_2		
DC	0.14	1.86
PC	0.29	1.71
PRC	0.09	1.90

higher energy (100) planes to lower energy (111) planes during zero current time (for PC) and reverse current time (for PRC) resulting in random texture in these coatings. Table

3.2 summarizes the results of texture coefficient calculations for the observed (111) and (200) reflections in pure nickel and nickel composite coatings. The texture coefficients for (111) and (200) reflections of standard randomly oriented polycrystalline sample (JCPDS: 04-0850) are unity. For all the coatings (except PRC codeposited Ni-ZrO_2), the (200) texture coefficient for DC deposition is greater than that for PC and PRC deposition indicating strong (100) crystallographic texture in these coatings. However, the (111) texture coefficients for all the coatings (except PRC deposited Ni-ZrO_2) are greater for PC and PRC deposition compared to that for DC deposition. This again indicates relatively random orientation in PC and PRC deposited coatings compared to DC deposition.

3.1.4 Microhardness and Wear Resistance:

The variation of microhardness of pure nickel and nickel composite (Ni-Al_2O_3, Ni-SiC, and Ni-ZrO_2) coatings with deposition conditions (DC, PC, and PRC) is presented in Fig. 3.5. In general, hardness of the coatings increases with this order of deposition conditions: DC, PC, and PRC. The improvement in the hardness of pure nickel coatings with PC and PRC deposition conditions is very small (<50 HV). This seems to be due to changes in crystallographic texture in pure nickel coatings with the deposition conditions. As discussed earlier, this order of deposition conditions (DC, PC, and PRC) also resulted in increasing content of reinforced nanoparticles in the coatings. Thus, the improvements in the hardness of composite coatings with PC and PRC deposition conditions seem to be due to increased content of reinforced hard particles in the coatings. Also, for all the

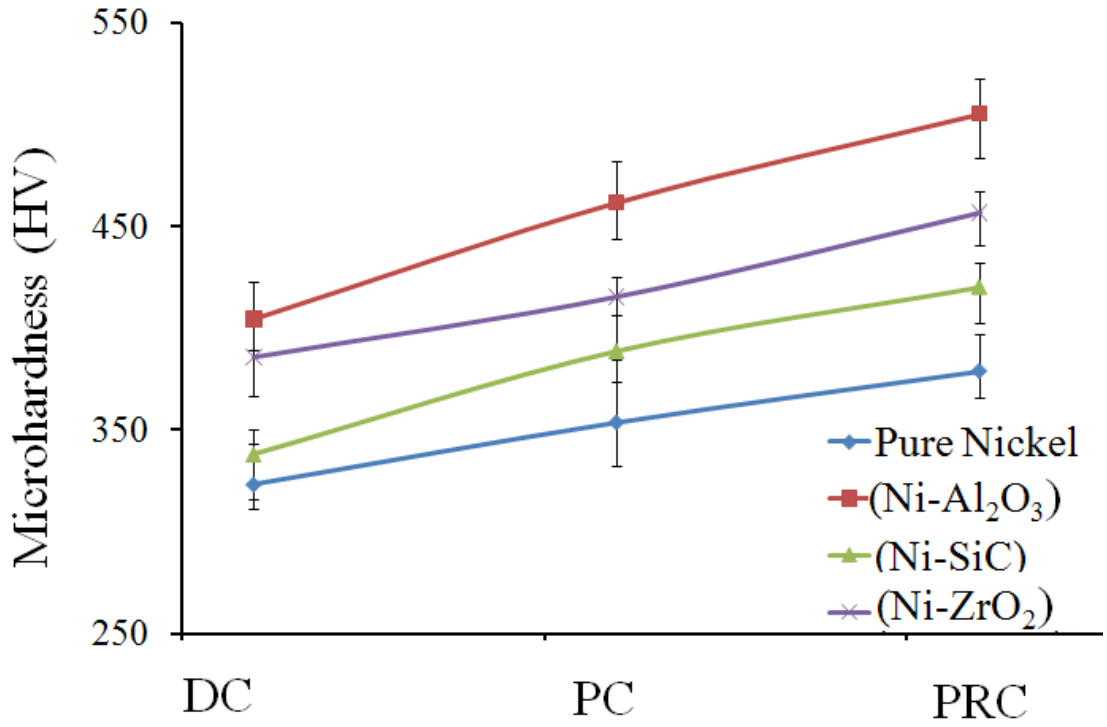

Fig. 3.5 *Microhardness of pure nickel and nickel composite coatings deposited by DC, PC and PRC electrodeposition methods*

deposition conditions, the hardness of composite coatings is higher than pure nickel coatings. This seems to be a direct consequence of dispersion strengthening effect where reinforced hard particles in the matrix obstruct the motion of dislocations. Furthermore, the Ni-Al_2O_3 composite coatings exhibit highest hardness and the Ni-SiC coatings exhibit lowest hardness for each deposition condition (DC, PC, and PRC). Note that SiC particles (hardness: ~22 GPa) are harder than Al_2O_3 (hardness: ~15 GPa) and ZrO_2 (hardness: ~13 GPa) particles. As such, the highest hardness of Ni-Al_2O_3 composite coatings seems to be due to relatively larger content of Al_2O_3 (in Ni- Al_2O_3) than SiC (in Ni-SiC) and ZrO_2 (in Ni-ZrO_2) in coatings for each deposition condition (Fig. 3.3).

The wear weight loss of pure nickel and nickel composite coatings (Ni-Al_2O_3, Ni-SiC, and Ni-ZrO_2) coatings with deposition conditions (DC, PC, and PRC) is presented Fig. 3.6. The pure nickel coatings for all the deposition conditions showed maximum weight loss compared to nickel composite coatings. This is a direct consequence of the lower microhardness of the pure nickel coatings compared to nickel composite coatings. Also, the Ni-Al_2O_3 composite coatings, which are hardest among all the composite coatings, showed least weight loss. For all the coatings, the wear weight loss was found to be decreased from DC to PC and PRC deposition conditions due to increasing hardness of the coatings (resulting from increasing reinforced nanoparticle content for composite coatings and texture related effects in pure nickel coatings).

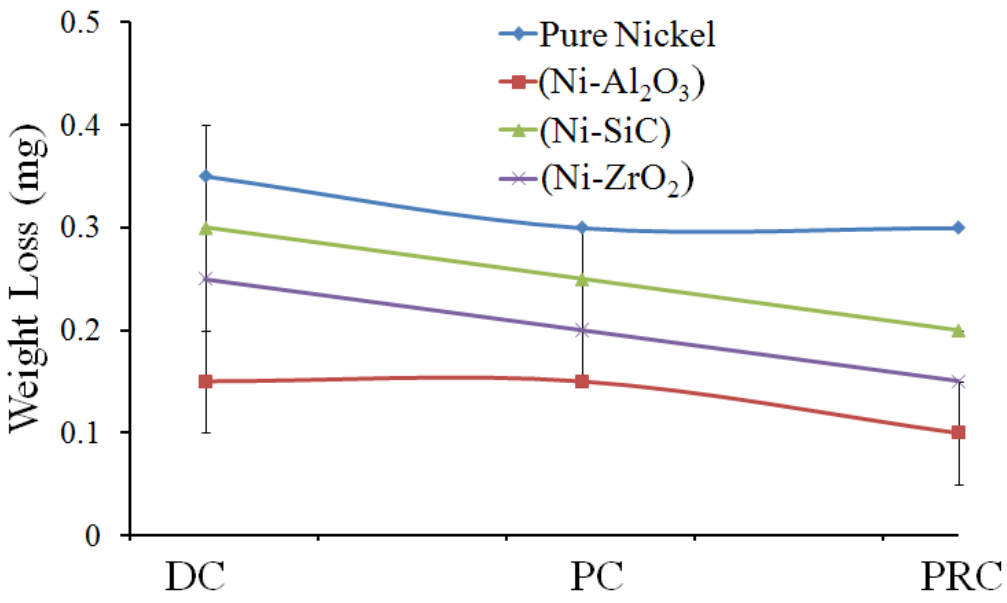

Fig. 3.6 *The variation of weight loss for pure nickel and nickel composite coatings deposited by DC, PC and PRC electrodeposition methods.*

3.2 Effect of Reinforcement Content on Microstructure and Properties of Ni-Al_2O_3 Composite Coatings

3.2.1 Coating Composition, Surface Morphology, and Thickness:

To understand the influence of reinforcement content on the microstructure and properties of composite coatings, several Ni-Al_2O_3 coatings were deposited by varying the content of Al_2O_3 nanoparticles in the electrolytic bath (5, 10, 20, and 40 g/L). The variation of Al_2O_3 content in the nickel composite coatings as a function of content of Al_2O_3 nanoparticles in the electrolytic bath is shown in Fig. 3.7. The wt.% of alumina in the composite coatings (deposited using similar electrodeposition parameters) significantly increases with increasing alumina content in the electroplating bath.

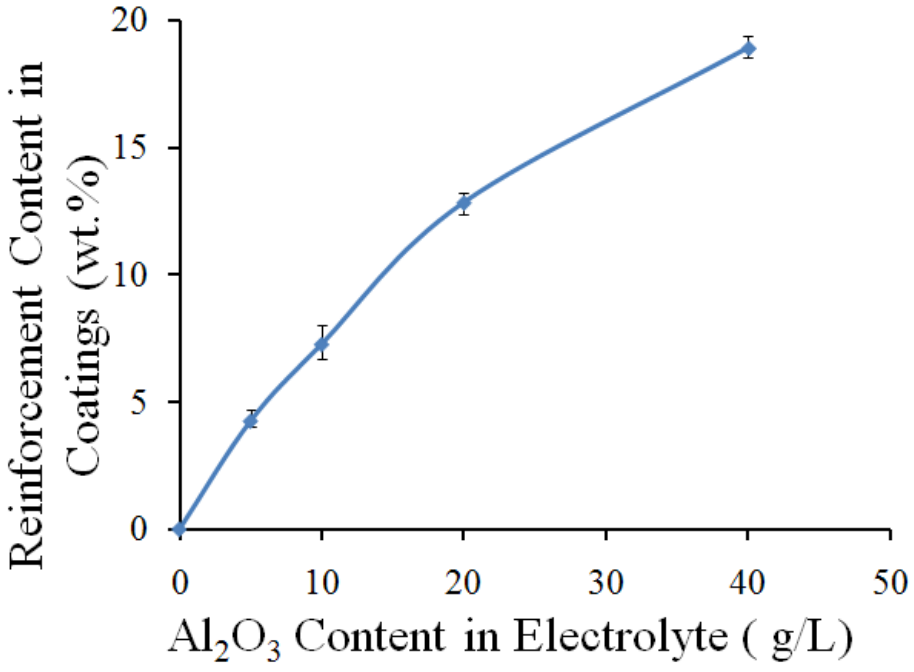

Fig. 3.7 *Wt.% of Al_2O_3 in the Ni-Al_2O_3 composite coatings as a function of nanoparticle content in the electrolyte bath.*

The surface morphologies of the pure nickel coating and Ni-Al_2O_3 composite coatings, deposited with varying content of Al_2O_3 nanoparticles in the electrolytic bath (5, 10, 20, and 40 g/L), are presented in Fig. 3.8. As the Al_2O_3 nanoparticles content increases the coating surfaces become increasingly inhomogeneous with appearance of coarser granular features. As such, the surface roughness of composite coatings increases with increasing Al_2O_3 reinforcement in the coatings (Fig. 3.9). The Ni-Al_2O_3 composite coatings deposited from electrolyte bath with 40 g/L alumina exhibited maximum surface roughness.

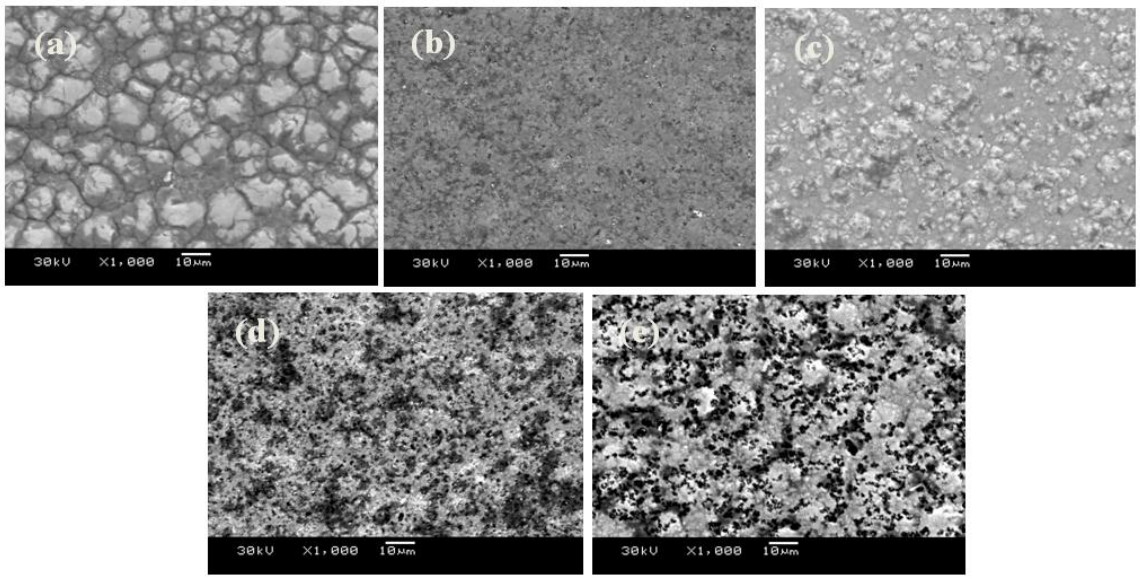

Fig. 3.8 *Surface micrographs from PC electrodeposited (a) pure nickel (0 g/L), (b) Ni-Al_2O_3 (5g/L), (c) Ni-Al_2O_3 (10g/L), (d) Ni-Al_2O_3 (20g/L), and (e) (Ni-Al_2O_3 (40g/L) coatings deposited from electrolyte bath with varying content of suspended nanoparticles.*

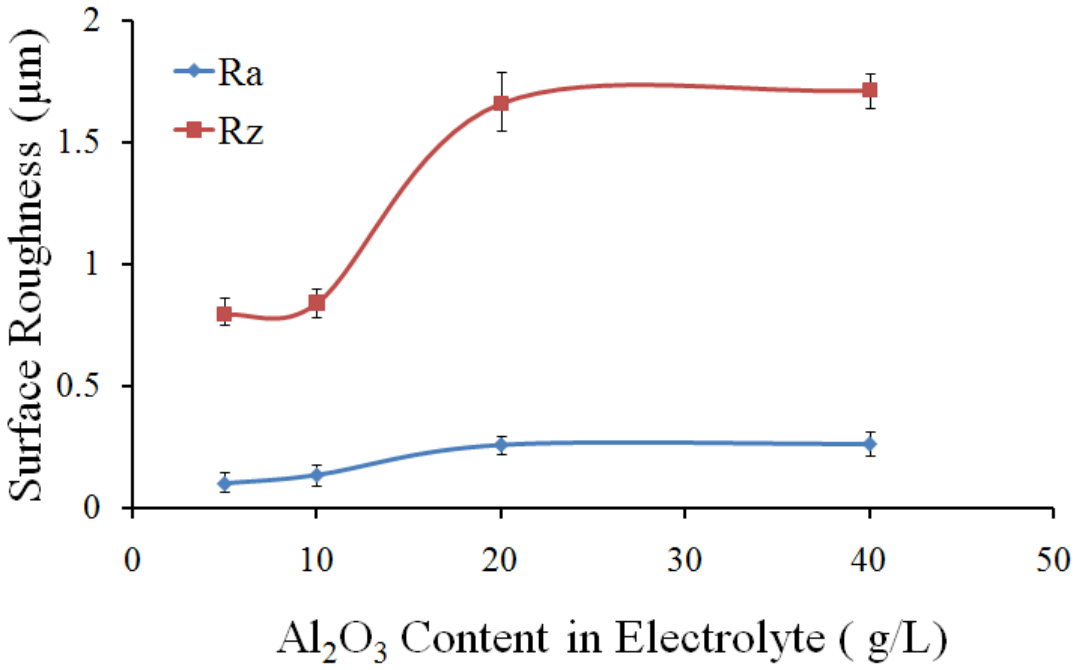

Fig. 3.9 *Surface roughness of nickel and Ni-Al_2O_3 composite coatings as a function of nanoparticle content in the electrolyte bath.*

The cross-sectional images of pure nickel and Ni-Al_2O_3 composite coatings deposited using similar pulse electrodeposition parameters are shown in Fig. 3.10. All the coatings were uniform, crack-free, and homogeneous. Interestingly, the pure nickel coatings were significantly thicker than Ni-Al_2O_3 composite coatings deposited using similar electrodeposition conditions (Fig. 3.11). Also, the thickness of composite coatings decreased with increasing alumina incorporation in the composite coatings. It seems that the reinforced alumina particles in the composite coatings act as physical barriers to grain growth and slow down the growth rate (hence thinner composite coatings).

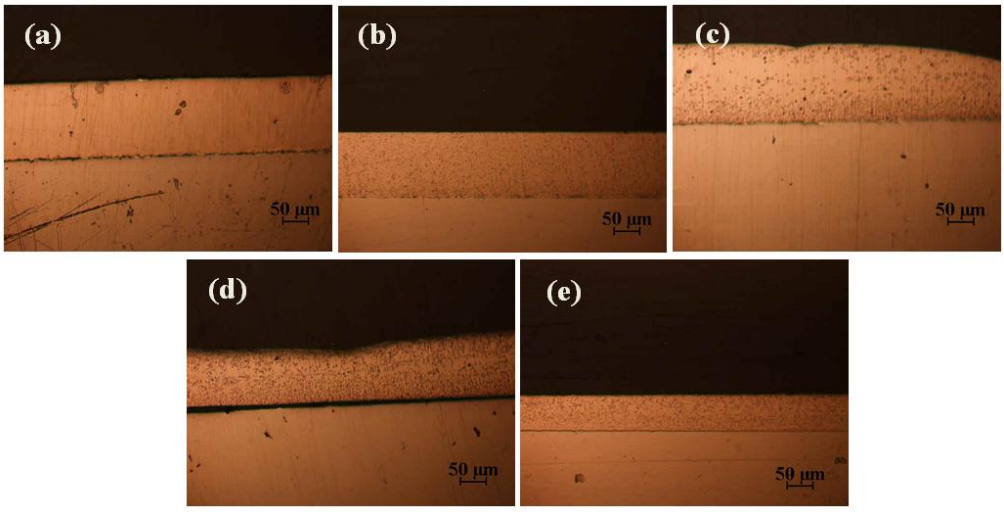

Fig. 3.10 *Cross-sectional images PC electrodeposited (a) pure nickel (0 g/L), (b) Ni-Al_2O_3 (5g/L), (c) Ni-Al_2O_3 (10g/L), (d) Ni-Al_2O_3 (20g/L), and (e) Ni-Al_2O_3 (40g/L) composite coatings deposited from electrolyte bath with varying content of suspended nanoparticles.*

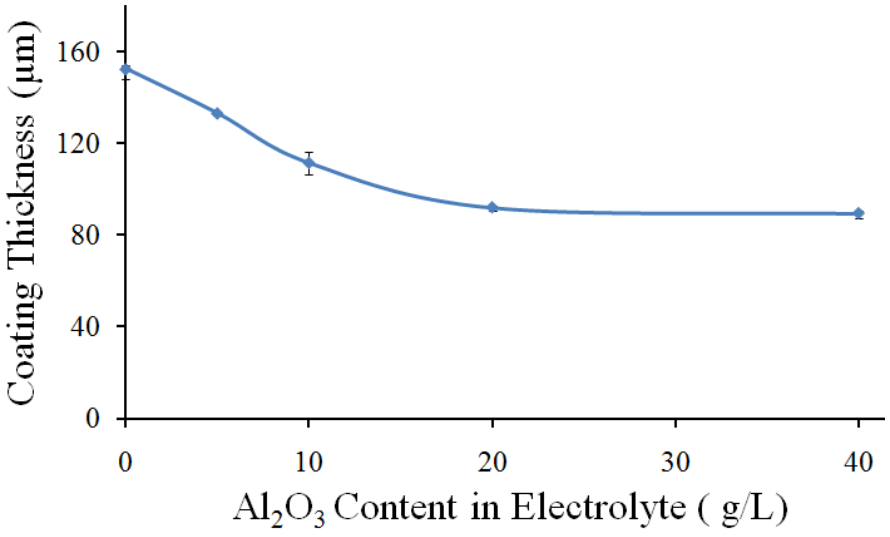

Fig. 3.11 *Variation of thickness of Ni-Al_2O_3 composite coatings with nanoparticle content in the electrolyte bath.*

3.2.2 Crystallographic Texture:

The x-ray diffraction (XRD) patterns of pure nickel and Ni-Al_2O_3 composite coatings, deposited with varying content of Al_2O_3 nanoparticles in the electrolytic bath are shown in Fig. 3.12. The XRD patterns show typical peaks corresponding to (111) and (200) crystallographic planes of pure nickel at 2θ positions 44.508° and 51.847°, respectively. Note that the peaks corresponding to reinforced Al_2O_3 nanoparticles could not be resolved in XRD patterns from composite coatings due to very small size of the nanoparticles and low reinforcement content. Detailed analysis of XRD patterns is necessary to understand effect of alumina reinforcement on the development of coating microstructure and microtexture.

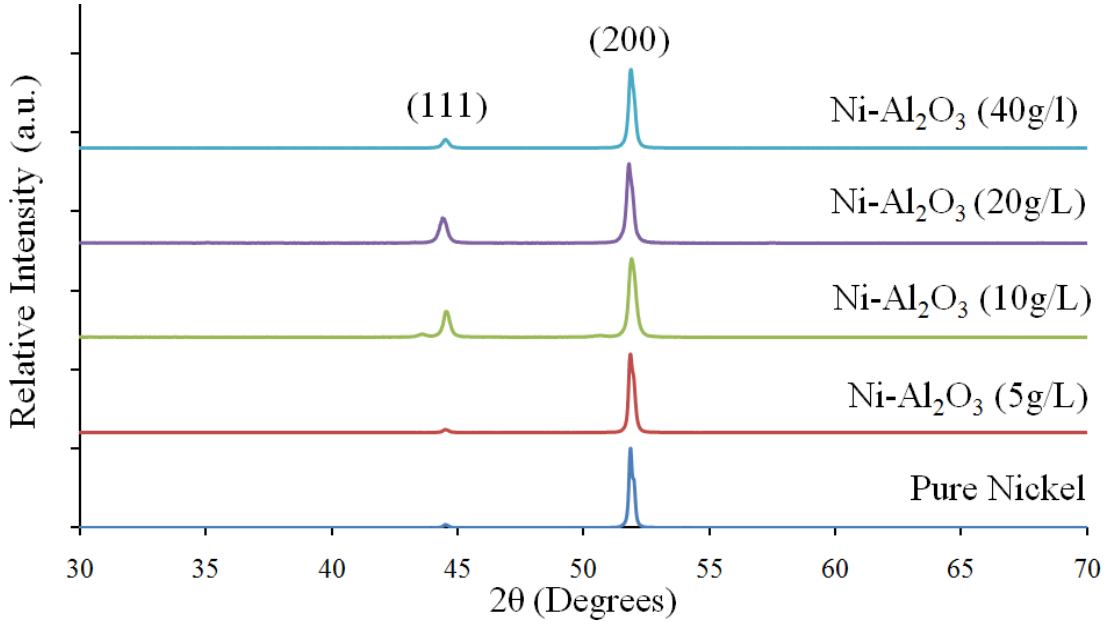

Fig. 3.12 *X-ray diffraction patterns from PC electrodeposited pure nickel and Ni-Al_2O_3 composite coatings deposited from electrolyte bath with varying content of suspended nanoparticles.*

The crystallite sizes for pure nickel and Ni-Al_2O_3 composite coatings, calculated from FWHM using Scherrer's equation, are presented in Table 3.3. For all the coatings, crystallite size of the nickel matrix is less than 40 nm. While the data shows slight decrease in crystallite size with incorporation of Al_2O_3 nanoparticles in the coating, this calculated data should be used only as general information. For more accurate analysis of the crystallite and grain size in nano-scale range, high resolution transmission electron microscopy (TEM) needs to be done. A careful analysis of XRD patterns also revealed distinct difference in the relative intensities of primary (*hkl*) peaks from nickel and Ni-Al_2O_3 composite coatings.

Table 3.3 Crystallite size and texture coefficients (TCs) of various (*hkl*) planes for standard sample, pure nickel, and Ni-Al_2O_3 composite coatings.

		Texture Coefficient (TC)	
Coatings	**Crystallite Size (nm)**	**(111)**	**(200)**
Standard Sample		1	1
Pure Nickel	38	0.03	1.97
Ni-Al_2O_3 (5g/L)	33	0.03	1.97
Ni-Al_2O_3 (10g/L)	31	0.24	1.76
Ni-Al_2O_3 (20g/L)	30	0.24	1.76
Ni-Al_2O_3 (40g/L)	27	0.09	1.91

As mentioned earlier, the standard randomly oriented polycrystalline nickel exhibits strongest peak corresponding to (111) crystallographic plane at 2θ=44.508° (JCPDS 04-0850). All the pure nickel and Ni-Al_2O_3 coatings exhibit strongest peak corresponding to (200) plane at $2\theta = 51.847°$ indicating development of crystallographic texture. However, as the Al_2O_3 nanoparticle content in the electrolyte increases up to 20 g/L, the intensity of (111) peak increases. This also corresponds to increasing values of (111) texture coefficient and decreasing values of (200) texture coefficients (Table 3.3). Since (111) peak is the strongest peak in the standard pattern of randomly oriented polycrystalline sample, the increasing intensity of this peak in the Ni-Al_2O_3 composite coatings indicates decreasing preferential orientation (or increasing randomness) with reinforcement content in the coating. It seems that reinforcement of alumina particles in nickel matrix prohibit grain growth of primary columnar grains (oriented in fastest growing [100] direction) and also provide nucleation sites for the growth of new randomly oriented grains. This also supports the observations of smaller thickness of Ni-Al_2O_3 composite coatings compared to pure nickel coatings deposited using similar pulse electrodeposition parameters. The Ni-Al_2O_3 composite coatings deposited from electrolyte bath with 40 g/L did not follow above trend, and exhibited the intensities of various planes and values texture coefficients similar to that for pure nickel coatings. This is probably due to agglomeration of nanoparticles during deposition at such high level of Al_2O_3 content in the electrolyte. Note that surface roughness of this composite coating was highest (Fig. 3.9).

3.2.3 Microhardness and Wear Resistance:

The variation of microhardness Ni-Al_2O_3 composite coatings as a function of Al_2O_3 nanoparticle content in the electrolytic bath is presented in Fig. 3.13. The microhardness of Ni-Al_2O_3 composite coatings is about 50-150 HV higher than pure nickel coatings, and the hardness increases with increasing alumina content in the electrolyte bath. The hardness of composite coatings is mainly determined by the microstructure of matrix and properties of reinforced particles in the coatings. Since all the coatings have nanocrystalline nickel matrix, the increasing hardness of the Ni-Al_2O_3 composite coatings with increasing alumina content in the electrolyte bath seems to be primarily due to enhanced dispersion strengthening effects.

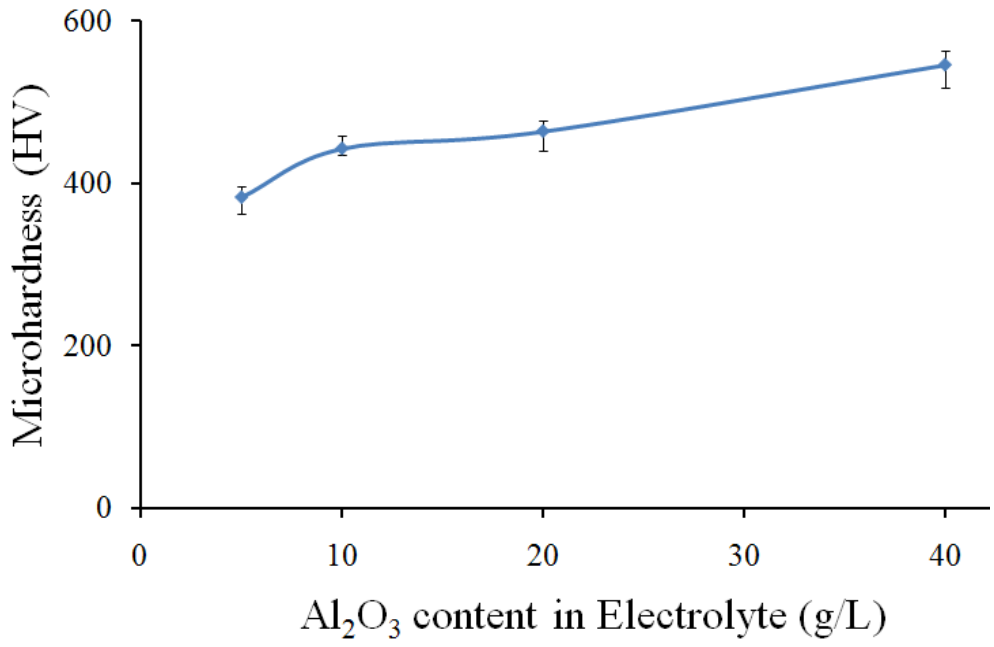

Fig. 3.13 *Variation of microhardness of Ni-Al_2O_3 composite coatings with nanoparticle content in the electrolyte bath.*

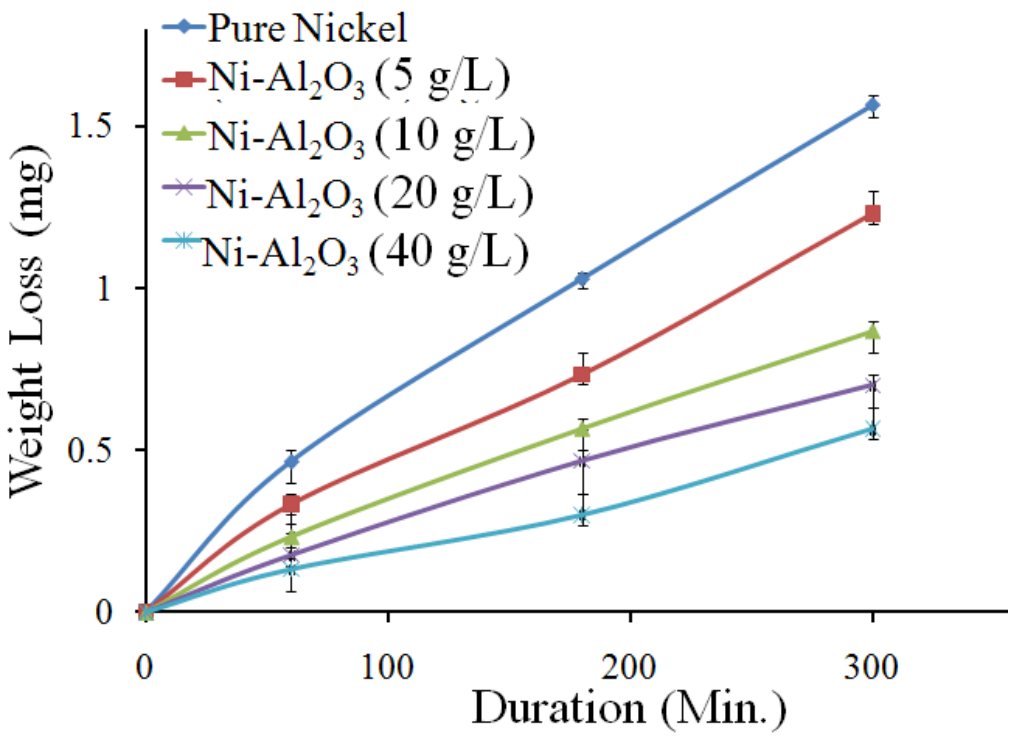

Fig. 3.14 *The variation of weight loss with time for pure nickel and nickel composite coatings deposited from electrolyte bath with varying content of suspended nanoparticles.*

The variation of cumulative weight loss as a function of wear time for nickel and Ni-Al_2O_3 composite coatings (deposited with varying content of Al_2O_3 nanoparticles in the electrolytic bath) is presented in Fig. 3.14. The relative wear behavior of all the coatings is in agreement with the general understanding that the harder coatings are more wear resistant. The pure nickel coatings showed severe weight loss compared to all the Ni-Al_2O_3 coatings. Furthermore, the wear resistance of the composite coatings improved with increasing content of Al_2O_3 nanoparticles in the electrolytic bath. Note that the microhardness of the Ni-Al_2O_3 composite coatings has increased with increasing content of Al_2O_3 nanoparticles in the electrolytic bath. These reinforced Al_2O_3 particles in nickel

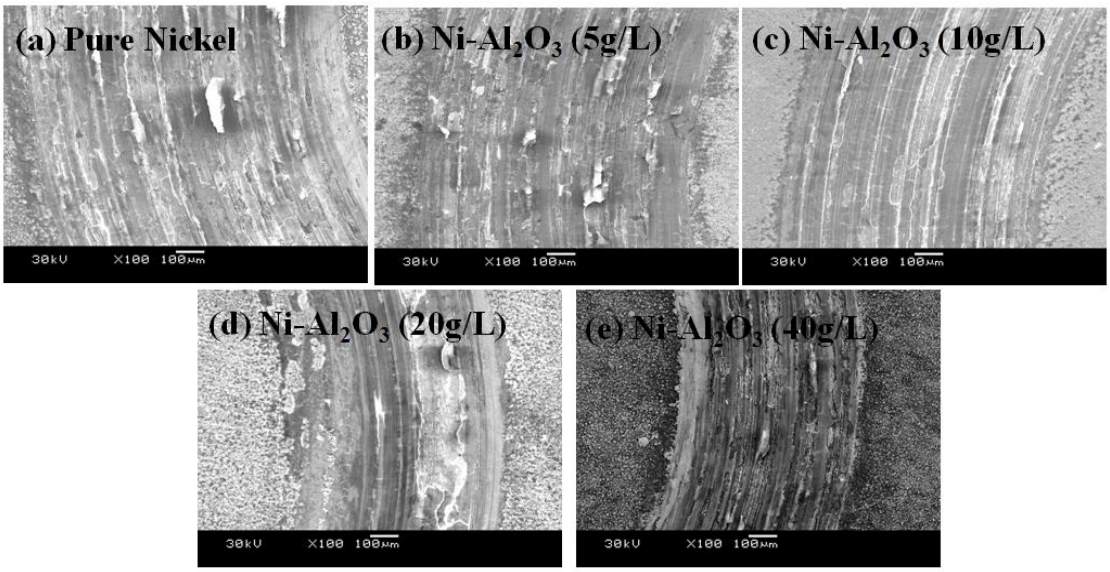

Fig. 3.15 *Morphology of worn surfaces of PC electrodeposited (a) pure nickel (0 g/L), (b) Ni-Al_2O_3 (5g/L), (c) Ni-Al_2O_3 (10g/L), (d) Ni-Al_2O_3 (20g/L), and (e) Ni-Al_2O_3 (40g/L) composite coatings deposited from electrolyte bath with varying content of suspended nanoparticles.*

matrix restrains the plastic deformation of matrix under loading due to dispersion strengthening effects. These effects become stronger with increasing alumina content in the composite coatings. These reinforced nanoparticles also lowers the adhesive wear between nickel matrix and alumina ball by reducing the direct contact between these counter bodies during the sliding. The SEM micrographs from wear tracks of pure nickel and Ni-Al_2O_3 composite coatings are presented in Fig. 3.15. The worn surface from pure nickel shows many continuous and wide grooves. The severe plastic deformation of the nickel under loading causes abrasive grooves parallel to sliding direction. The formation of wide grooves and plastic deformation are indicative of poor wear resistance of pure nickel coatings. As the nanoparticle content in the Ni-Al_2O_3 composite coatings

increases, the wear grooves on the wear surfaces become progressively discontinuous indicative of increased resistance to plastic deformation. For coatings with higher nanoparticle content, for example the coating deposited from electrolyte bath with 20 g/L Al_2O_3 nanoparticles), the micro-cracking on the wear surface of the coatings is clearly visible. Furthermore, the width of the wear tracks progressively decreases with increasing Al_2O_3 reinforcement content in the composite coatings which is indicative of better wear resistance of these coatings. Fig. 3.16 shows the variation of coefficient of friction with time for pure nickel and Ni-Al_2O_3 coatings.

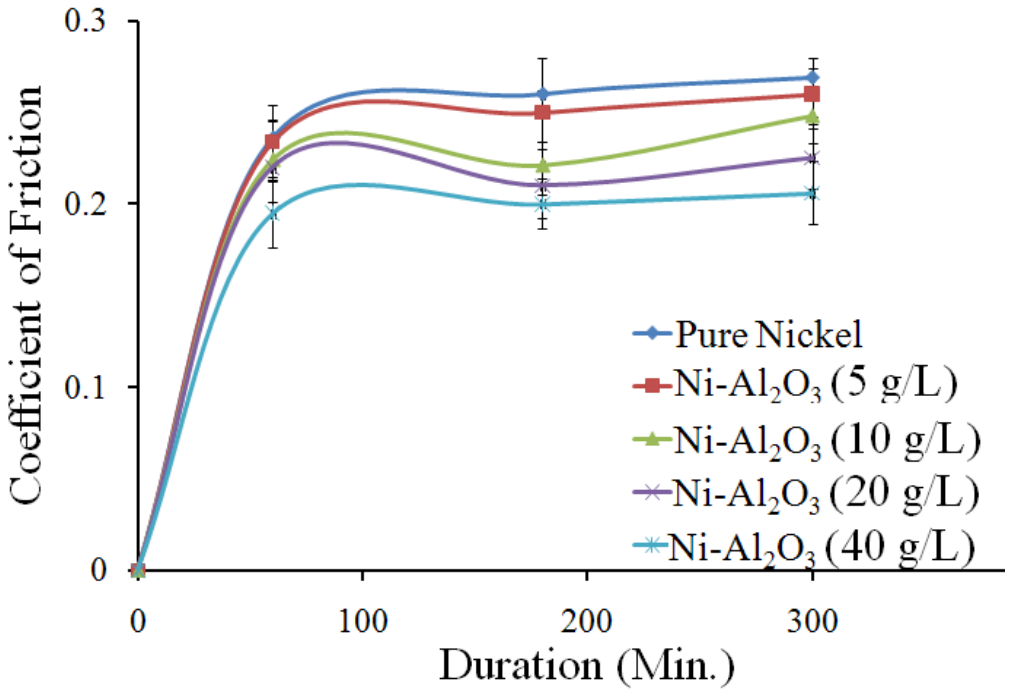

Fig. 3.16 *Variation of coefficient of friction with sliding time for pure nickel and nickel-alumina composite coatings.*

For all the coatings, the coefficient of friction increases with time (<50 min) and quickly stabilizes to steady state value. While the average coefficient of friction decreases with increasing reinforcement content in the Ni-Al_2O_3 composite coatings, the variation is not significant and the coefficient of friction for all the coatings ranges between ~0.2-0.25.

3.3 Pulse electrodeposition of Ni-CNT Composite Coatings

3.3.1 Microstructure Analysis

The cross-sectional images of pure nickel coating and Ni-CNT composite coatings deposited using same pulse electrodeposition parameters are presented in Fig. 3.17. This figure indicates that the coatings are uniform in thickness and exhibit very good bonding with the substrate. Even though the electrodeposition parameters were same, the thickness of pure nickel coatings (19±0.5 μm) was observed to be almost two times the thickness of Ni-CNT composite coatings (9±0.5 μm). It seems that the reinforcement of the CNTs in the nickel matrix prohibit the normal columnar growth of the crystal (perpendicular to the substrate surface). The subsequent random nucleation of nickel on the CNTs and growth in off-normal direction results in the decrease in effective growth rate in normal direction (and hence less coating thickness in given electrodeposition time). This is further explained in the following sections.

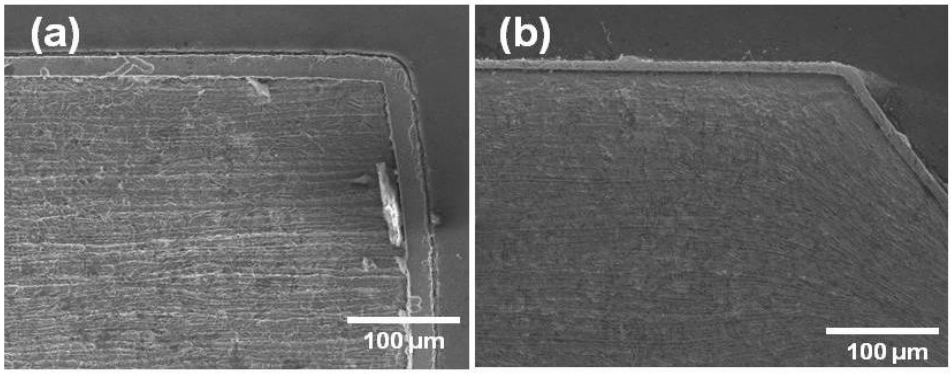

Fig. 3.17 *SEM images of cross-section of (a) pure nickel coating, (b) Ni-CNT composite coating. All coatings were pulse electrodeposited using same pulse parameters.*

Typical SEM micrographs from the surface of the pure nickel coating are presented in Fig. 3.18 (a) and (b). The nickel coating exhibits the smoothest and most compact microstructure. The surface structure of the pure nickel coating is made up of regular pyramidal crystals with uniform grain size. High instantaneous current density during pulse electrodeposition helps to enhance the nucleation rate which leads to the formation of finer grains. The Fig. 3.18 (c) and (d) show SEM images of the Ni-CNT composite coating with proper pretreatment of CNTs with nitric acid. While the distribution of dispersed CNTs (single CNT) is very difficult to observe though more uniform fiber like CNTs network observed throughout the surface which always have better surface morphology than CNTs bundles.

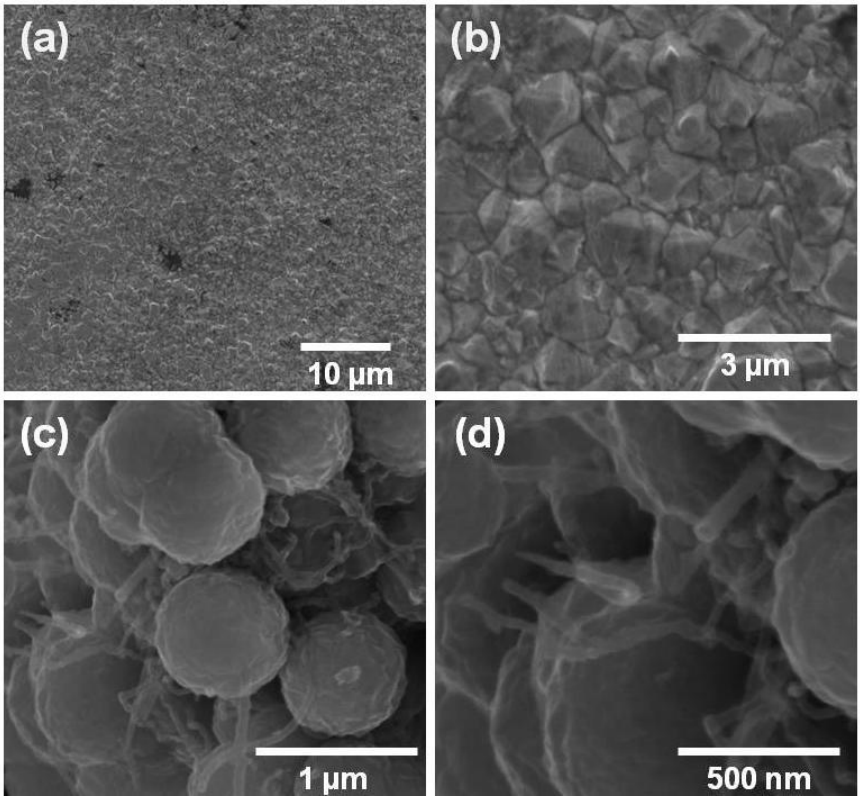

Fig. 3.18 *SEM images of (a),(b) pure nickel coating, (c),(d) Ni-CNT composite coating. All coatings were pulse electrodeposited using same pulse parameters.*

3.3.2 Phase Analysis

The x-ray diffraction (XRD) patterns for pure nickel and Ni-CNT composite coatings obtained from different plating bath are shown in Fig. 3.19. The XRD patterns show typical peaks corresponding to (111), (200), and (220) crystallographic planes of nickel. To understand the influence of CNT reinforcement on the development of coating microstructure and micro-texture, detailed analysis of XRD patterns was conducted.

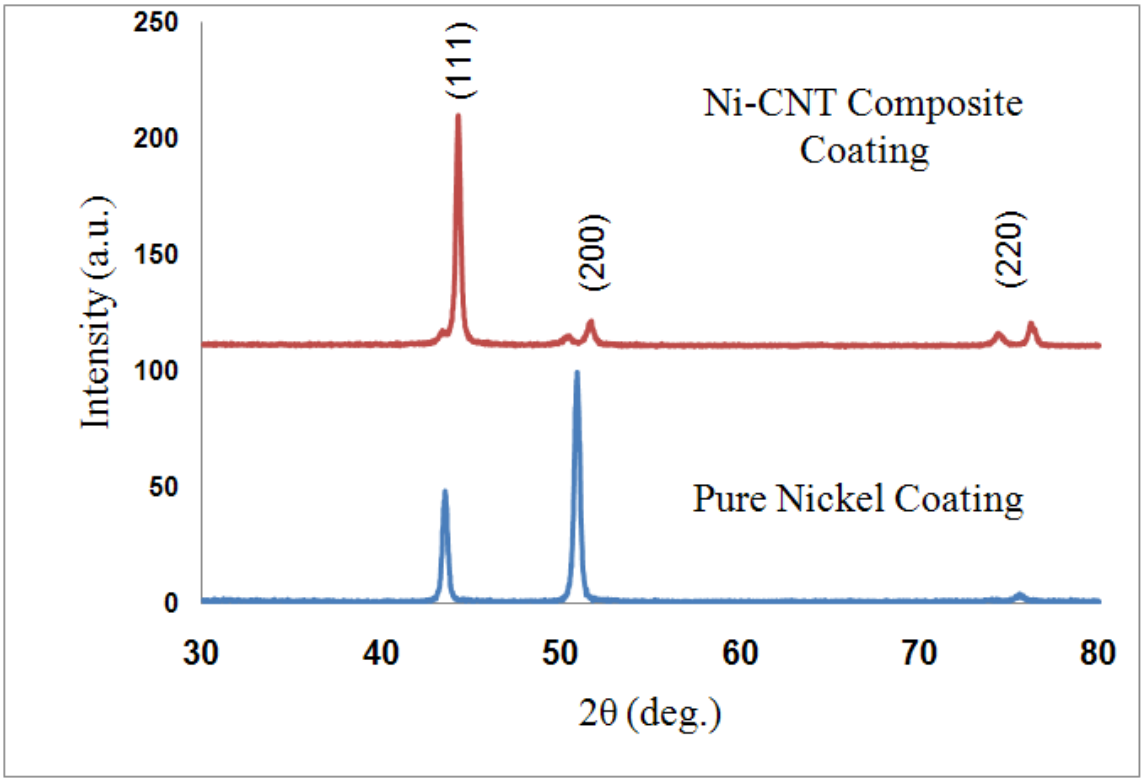

Fig. 3.19 *X-ray diffraction patterns from pure nickel coating and Ni-CNT composite coating electrodeposited using same pulse parameters.*

First, the crystallite size was calculated for both pure nickel and Ni-CNT composite coatings using Scherrer's equation. Table 3.4 shows crystallite sizes of pure nickel as well as Ni-CNT composite coatings calculated using FWHM of prominent (111) reflection in Scherrer's equation. The calculated crystallite size for pure nickel coating was 37 nm, which is significantly greater than that in Ni-CNT composite coatings (28 nm). This indicates that the reinforcement of CNTs in the nickel resulted in refinement of the microstructure of the composite coatings.

Table 3.4 Crystallite size and texture coefficients of various (*hkl*) planes for pure nickel and Ni-CNT composite coatings.

		Texture Coefficients		
	Crystallite Size (nm)	**(1 1 1)**	**(2 0 0)**	**(2 2 0)**
Pure Nickel coating	37	0.47	2.32	0.20
Ni-CNT composite coating	28	1.67	0.47	0.87

Careful analysis of the x-ray diffraction data also revealed the distinct difference in the relative intensities of some of the (*h k l*) peaks in XRD patterns of Ni and Ni-CNT composite coating. The standard randomly oriented polycrystalline nickel exhibits strongest peak corresponding to (111) plane at $2\theta = 44.508°$ (JCPDS 04-0850). The pure nickel coating in the present investigation exhibited strongest peak corresponding to (200) plane at $2\theta = 51.847°$ indicating development of crystallographic texture. Apparently [100] is the preferred grain growth direction for face centered cubic crystals. It seems that the growth of pure nickel coatings occurs by nucleation on the substrate surface followed by growth of grains in preferred crystallographic direction i.e. [100]. These columnar grains eventually terminate at the coating surface resulting in pyramidal surface grain structure associated with (200) crystallographic texture [93]. In case of Ni-CNT composite coatings, the strongest peak corresponds to (111) plane at $2\theta = 44.508°$. This peak is also the strongest peak in XRD pattern from standard randomly oriented polycrystalline nickel. This indicates that the grain structure in Ni-CNT composite coating is more random. To quantify the crystallographic textures associated with nickel and Ni-CNT coatings, texture coefficients (TC) for predominant (h k l) peaks in XRD

patterns were calculated. (111), (200), and (220) reflections were considered for texture coefficient calculation (n=3). Table 2 summarizes the results of texture coefficient calculations for the observed (h k l) reflection in nickel and CNT composite coatings. The texture coefficient of 1 for any (h k l) represents standard randomly oriented polycrystalline sample. The texture coefficient for (200) plane for pure nickel coating is significantly greater than texture coefficients for other planes, i.e. (111) and (220), clearly indicating the development of strong crystallographic texture corresponding to (200) or (100) planes.

For the composite Ni-CNT coatings, the texture coefficients for (200) and (220) planes are close to one indicating predominantly random orientation of grains. Since texture coefficient for (111) plane is greater than 1, there is possibility of weak (111) texture in the Ni-CNT coatings. The schematic showing effect of CNTs on the development of texture and thickness of the coating is presented in Fig. 3.20. It seems that the co-deposition of CNTs in the nickel matrix prohibit the grain growth of columnar grains and also provides the nucleation sites for the growth of new grains. Depending on the orientation of the CNTs, the newly nucleated grains would grow along preferred [100] direction which may not be perpendicular to the substrate (possibly perpendicular to the CNT axis). This will further preclude the growth of surrounding columnar grains. The complexity of the grain nucleation and growth in presence of CNTs seems to result in more random grain structure or weak (111) texture in the Ni-CNT composite coating. This repeated nucleation and off-normal growth of nickel in presence of CNTs not only results in random/weak crystallographic texture but also decreases the effective growth rate in normal direction (perpendicular to substrate). This also supports the observation of

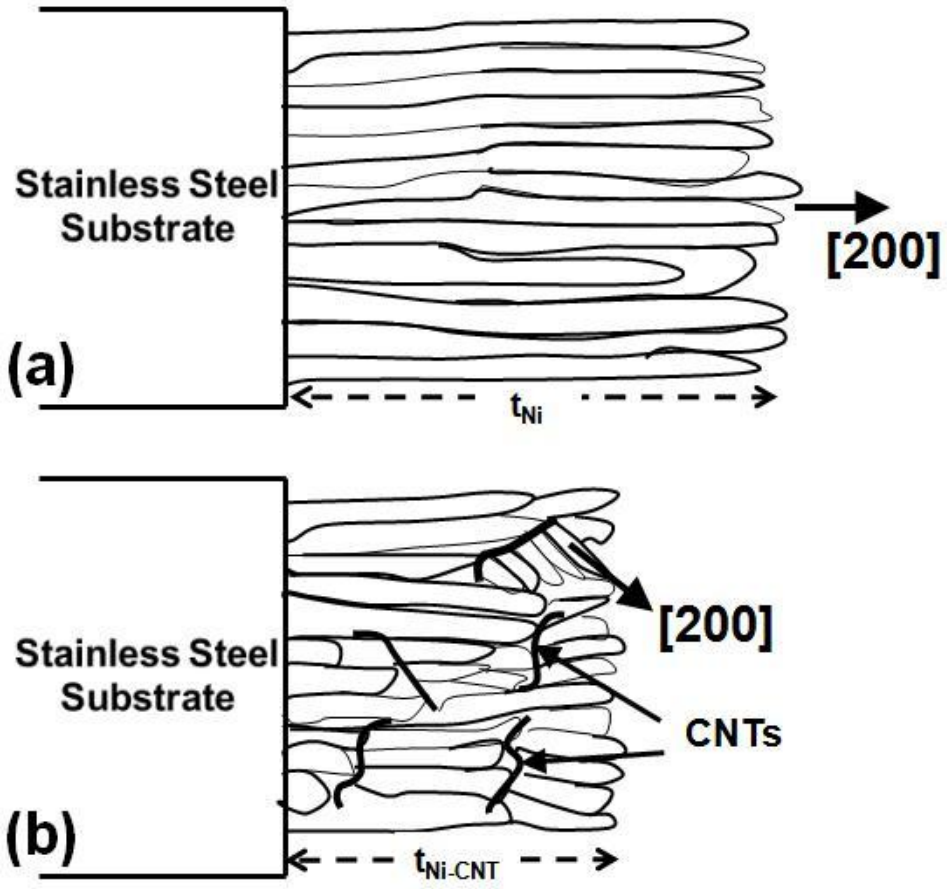

Fig. 3.20 *Schematic of the development of crystallographic texture and thickness in (a) pure nickel, and (b) Ni-CNT composite coatings deposited using same pulse electrodeposition parameters.*

smaller thickness of Ni-CNT composite coatings compared to pure nickel coatings ($t_{Ni\text{-}CNT} < t_{Ni}$) deposited using same pulse electrodeposition parameters.

3.3.3 Microhardness

The microhardness of pulse electrodeposited pure nickel coating and Ni-CNT composite coatings using same pulse parameters are presented in Fig. 3.21. The average microhardness of pure nickel coating was 320±15 HV. The hardness increased to 580±15 HV in case of Ni-CNT composite coatings deposited with nitric acid pretreatment of CNTs.

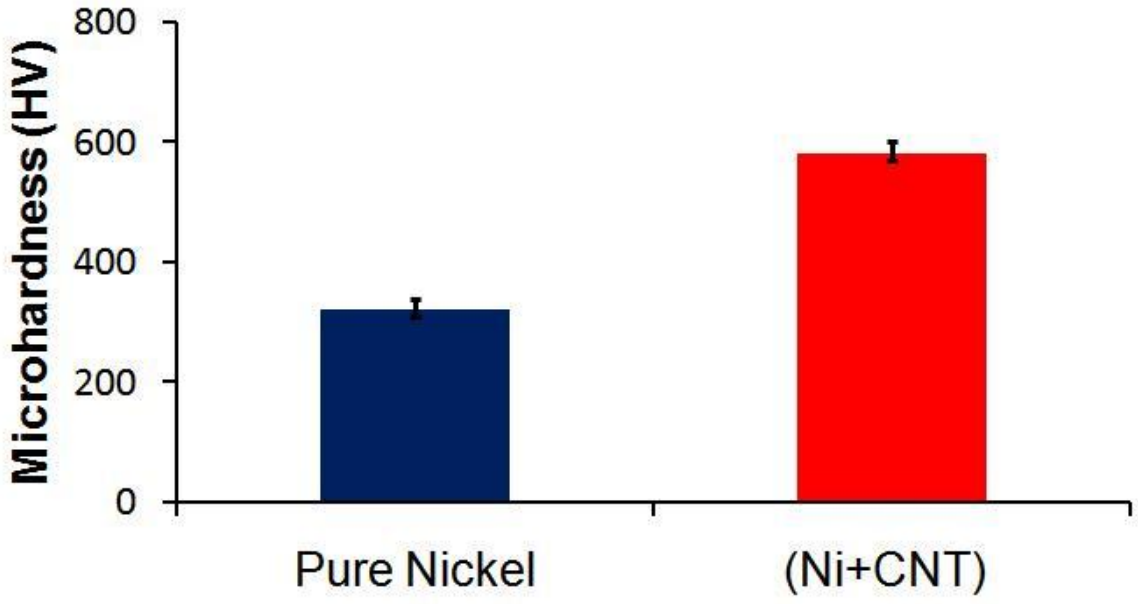

Fig. 3.21 *Microhardness of pulse electrodeposited pure nickel and Ni-CNT composite coatings.*

This remarkable increase in microhardness of Ni-CNT composite coatings can be resulting from a combination of Orowan strengthening as well as Hall-Petch strengthening. In the case of Ni-CNT composites, the Orowan strengthening is expected to involve bowing of the gliding dislocation between impenetrable carbon nanotubes and bypassing them, leaving behind dislocation loops. The refinement of nickel crystallite size due to CNT reinforcement (as discussed earlier) is also expected to increase the hardness owing to Hall-Petch strengthening.

3.3.4 Wear Resistance

The wear weight loss data for pure nickel coating and Ni-CNT composite coatings is presented in Fig. 3.22.

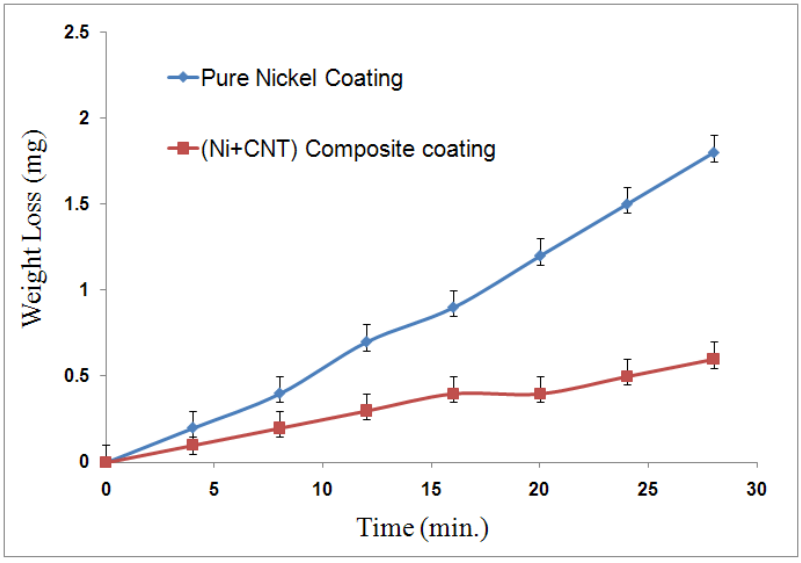

Fig. 3.22 *The variation of weight loss with time for pure nickel and Ni-CNT composite coatings.*

With the explored wear testing parameters in this investigation, the pure nickel coatings exhibit almost linear wear loss with time. The Ni-CNT composite coatings display significant improvement in the wear resistance compared to pure nickel coatings as indicated by the significantly lesser weight loss. The total weight loss in pure nickel coating is almost three times the total weight loss in Ni-CNT composite coating. It seems that better wear resistance of Ni-CNT composite coatings compared to pure nickel coating is a direct consequence of increase in surface hardness of the coatings.

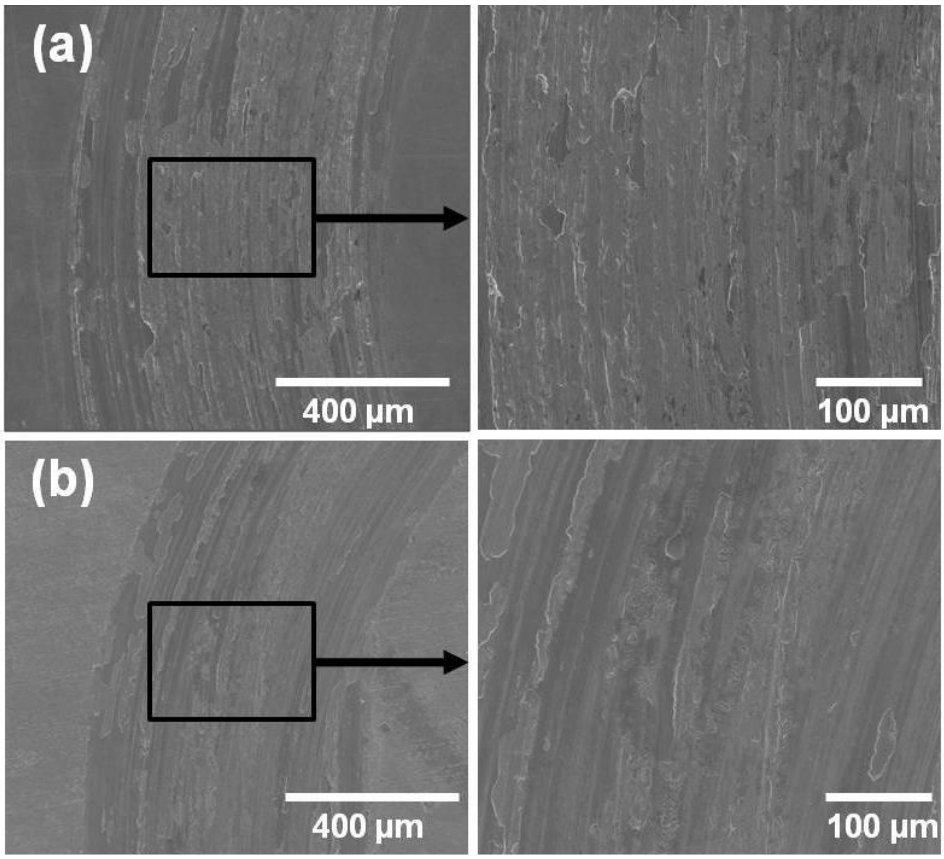

Fig. 3.23 *Worn surface morphology under dry sliding condition of (a) pure nickel coating, (b) Ni-CNT composite coating. All coatings were pulse electrodeposited using same pulse parameters.*

The SEM micrographs from the wear tracks of pure nickel and Ni-CNT composite coatings are presented in Fig. 3.23. The worn surface from pure nickel shows many continuous and wide grooves as well as severe plastic deformation (Fig. 3.23 (a)). The formations of wide grooves as well as plastic deformations are indicative of severe wear situation leading to poor wears resistance of pure nickel coating. The morphologies of wear tracks from Ni-CNT composite coating are shown in Fig. 3.23 (b). The worn surfaces of composite coatings shows discontinuous scratches associated with significantly lesser weight loss. The CNTs dispersed in the nickel matrix seems to prohibit the plastic deformation during wear. Due to the absence of severe plastic deformation, the wear resistance of Ni-CNT composite coating is significantly better than pure nickel coating. The uniform dispersion of CNTs into nickel matrix leads to significant increased in microhardness as well as wear resistance of (Ni+CNT) composite coatings.

3.3.5 Raman Spectroscopy Analysis

The Raman spectra of Ni-CNT composite coatings are illustrated in Fig. 3.24 and Fig. 3.25. The D and G band of CNTs are observed typically at 1353.7 cm^{-1} and 1585.5 cm^{-1} respectively. The G' band observed at 2709.6 cm^{-1}. This results clearly indicates the reinforcement of MWCNTs in the nickel composite coatings which is very difficult to determine using SEM and EDS methods.

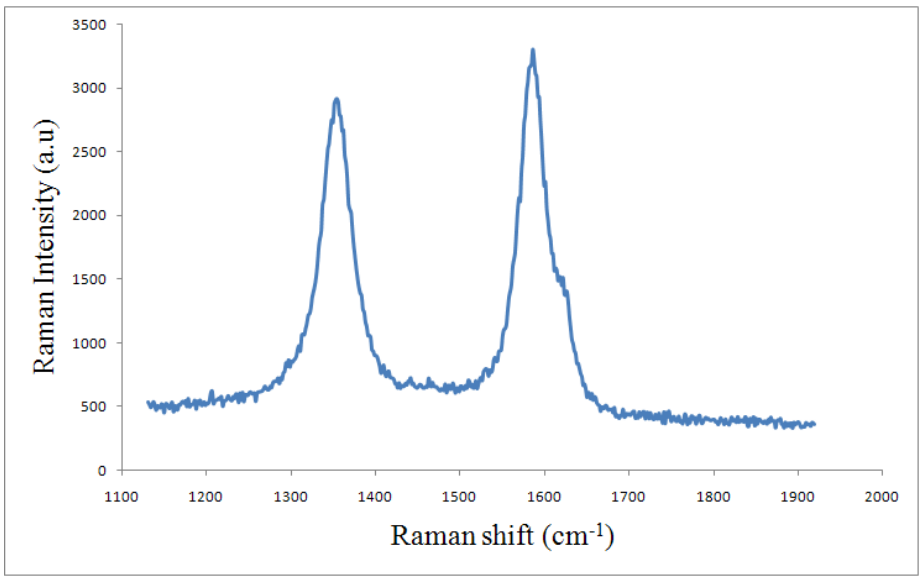

Fig. 3.24 *The Raman spectra of MWCNT, Ni-CNT composite coatings.*

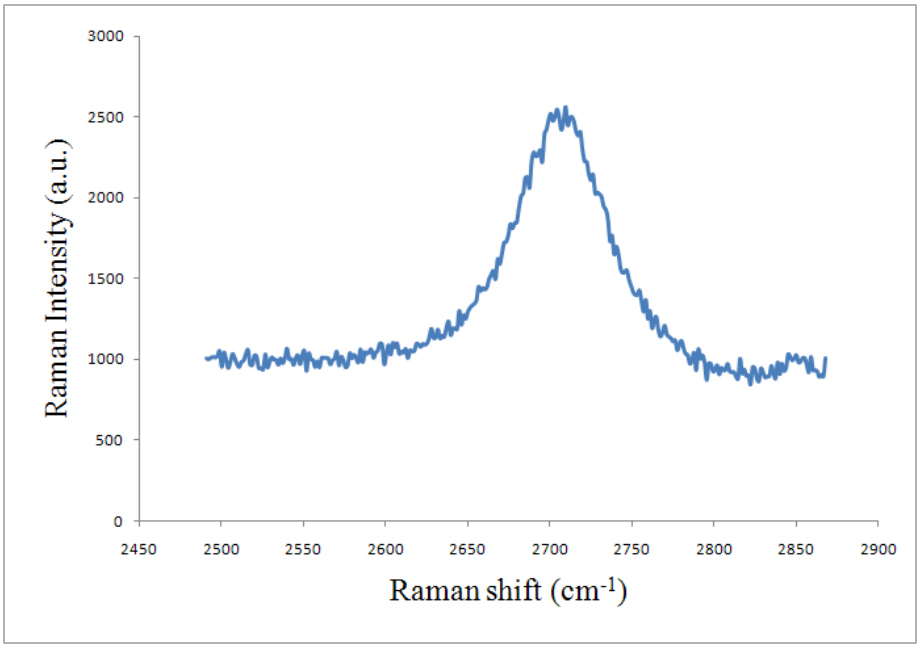

Fig. 3.25 *The Raman spectra of MWCNT, Ni-CNT composite coatings.*

CHAPTER 4

CONCLUSIONS

4.1 Effect of Plating Conditions (DC, PC, PRC) on Microstructure and Properties of Pure Nickel and Nickel Composite Coatings (Ni, Ni-Al_2O_3, Ni-SiC, and Ni-ZrO_2)

- For all the composite coatings (Ni-Al_2O_3, Ni-SiC, and Ni-ZrO_2), the amount of reinforcement in the coating was increased with PC and PRC deposition as compared to DC deposition.

- All the pure nickel and nickel composite coatings prepared using PC and PRC deposition exhibited more random/weak crystallographic textures compared to those deposited using DC deposition.

- For all the electrodeposition conditions (DC, PC, and PRC), the composite coatings (Ni-Al_2O_3, Ni-SiC, and Ni-ZrO_2) had significantly improved microhardness and wear resistance compared to pure nickel coatings.

- For each electrodeposition condition (DC, PC, or PRC), Ni-Al_2O_3 composite coatings exhibited better microhardness and wear resistance compared to Ni-SiC and Ni-ZrO_2 composite coatings due to relatively higher content of Al_2O_3 reinforcement in the coatings.

4.2 Effect of Reinforcement Content on Microstructure and Properties of Ni-Al_2O_3 Composite Coatings

- The reinforcement content of Al_2O_3 in the composite coatings increased with increasing content of nanoparticle loading in the electrolyte bath (up to 40 g/L).
- Except with the coatings deposited from electrolyte bath with 40 g/L nanoparticle content, the Ni-Al_2O_3 composite coatings showed relatively random/weak crystallographic texture compared to pure nickel coatings.
- For similar electrodeposition condition (PC), the Ni-Al_2O_3 composite coatings were thinner compared to pure nickel coatings due to more random/weak crystallographic texture in composite coatings.
- The microhardness and wear resistance of the Ni-Al_2O_3 composite coatings increased with increasing content of reinforced nanoparticles in the coatings (and also the content of nanoparticle loading in the electrolyte bath) due to enhanced dispersion strengthening effects.

4.3 Pulse electrodeposition of Ni-CNT composite coatings

- Pure Nickel and Ni-CNT composite coatings were successfully fabricated using pulse electrodeposition process employing Watts bath. The reinforcement of CNTs in the composite coating prohibited the columnar growth of the nickel grains resulting in random/weak texture and smaller coating thickness in the composite coatings.

- The CNT reinforcement further refined the crystallite size in the composite coatings. The Ni-CNT composite coatings exhibited significantly improved microhardness (580±15 HV) compared to pure nickel coatings (320±15 HV) primarily due to a combination of Hall-Petch and Orowan strengthening mechanisms.
- The pin-on-disc wear testing data indicated that the reinforcement of CNTs significantly improved wear resistance of the composite coating compared to pure nickel coatings.

4.4 Future work

Detailed analysis on microstructure growth of composite coatings by varying pulse parameters (Current density, duty cycle, and frequency) and by varying the incorporation of nanoparticles in the composite coatings. Development of graded composite coatings by combining DC, PC, and PRC electrodeposition methods as well as by varying pulse parameters. Corrosion study of composite coatings and detailed analysis on the effect of pulse parameters and reinforcement of nanoparticles in the coatings on corrosion behavior of the composite coatings is to be done. Effect of pulse parameters on mechanical and tribological properties of composite coatings. Quantitative analysis of nickel composite coatings needs to be done with the help of x-ray diffraction techniques using pole figure method.

REFERENCES

[1] A. M. El-Sherik and U. Erb, "Synthesis of bulk nanocrystalline nickel by pulsed electrodeposition," *Journal of Materials Science*, vol. 30, pp. 5743-5749, 1995.

[2] W. A. Aperador Chaparro and E. V. Lopez, "Electrodeposition of nickel plates on copper substrates using PC y PRC," *Matéria (Rio de Janeiro)*, vol. 12, pp. 583-588, 2007.

[3] A. Balasubramanian, *et al.*, "Effect of pulse parameter on pulsed electrodeposition of copper on stainless steel," *Surface Engineering*, vol. 25, pp. 389-392.

[4] F. Ebrahimi, *et al.*, "Mechanical properties of nanocrystalline nickel produced by electrodeposition," *Nanostructured Materials*, vol. 11, pp. 343-350, 1999.

[5] N. S. Qu, *et al.*, "Pulse electrodeposition of nanocrystalline nickel using ultra narrow pulse width and high peak current density," *Surface and Coatings Technology*, vol. 168, pp. 123-128, 2003.

[6] T. Song and D. Y. Li, "Tribological, mechanical and electrochemical properties of nanocrystalline copper deposits produced by pulse electrodeposition," *Nanotechnology*, vol. 17, p. 65, 2006.

[7] G. Devaraj, *et al.*, "Pulse plating," *Materials Chemistry and Physics*, vol. 25, pp. 439-461, 1990.

[8] M. S. Chandrasekar and M. Pushpavanam, "Pulse and pulse reverse plating--Conceptual, advantages and applications," *Electrochimica Acta,* vol. 53, pp. 3313-3322, 2008.

[9] L. Chen, *et al.*, "Influence of pulse frequency on the microstructure and wear resistance of electrodeposited Ni-Al_2O_3 composite coatings," *Surface and Coatings Technology,* vol. 201, pp. 599-605, 2006.

[10] M. Stroumbouli, *et al.*, "Codeposition of ultrafine WC particles in Ni matrix composite electrocoatings," *Surface and Coatings Technology,* vol. 195, pp. 325-332, 2005.

[11] S. Ding, *et al.*, "Pulse electrodeposition and nanoindentation test of ZrO_2/Ni nanocomposite," *Journal of Wuhan University of Technology--Materials Science Edition,* vol. 22, pp. 462-465, 2007.

[12] A. Möller and H. Hahn, "Synthesis and characterization of nanocrystalline Ni/ZrO_2 composite coatings," *Nanostructured Materials,* vol. 12, pp. 259-262, 1999.

[13] S.-L. Kuo, *et al.*, "Nano-particles dispersion effect on Ni/Al_2O_3 composite coatings," *Materials Chemistry and Physics,* vol. 86, pp. 5-10, 2004.

[14] N. K. Shrestha, *et al.*, "Composite coatings of nickel and ceramic particles prepared in two steps," *Surface and Coatings Technology,* vol. 140, pp. 175-181, 2001.

[15] L. Benea, *et al.*, "Wear corrosion properties of nano-structured SiC-nickel composite coatings obtained by electroplating," *Wear*, vol. 249, pp. 995-1003, 2001.

[16] S. K. Kim and H. J. Yoo, "Formation of bilayer Ni-SiC composite coatings by electrodeposition," *Surface and Coatings Technology*, vol. 108-109, pp. 564-569, 1998.

[17] C. T. J. Low, *et al.*, "Electrodeposition of composite coatings containing nanoparticles in a metal deposit," *Surface and Coatings Technology*, vol. 201, pp. 371-383, 2006.

[18] M. Musiani, "Electrodeposition of composites: an expanding subject in electrochemical materials science," *Electrochimica Acta*, vol. 45, pp. 3397-3402, 2000.

[19] A. F. Zimmerman, *et al.*, "Pulse electrodeposition of Ni-SiC nanocomposite," *Materials Letters*, vol. 52, pp. 85-90, 2002.

[20] A. F. Zimmerman, *et al.*, "Mechanical properties of nickel silicon carbide nanocomposites," *Materials Science and Engineering A*, vol. 328, pp. 137-146, 2002.

[21] P. Nowak, *et al.*, "Electrochemical investigation of the codeposition of SiC and SiO_2 particles with nickel," *Journal of Applied Electrochemistry*, vol. 30, pp. 429-437, 2000.

[22] K. H. Hou, *et al.*, "The wear behaviour of electro-codeposited Ni-SiC composites," *Wear,* vol. 253, pp. 994-1003, 2002.

[23] N. S. Qu, *et al.*, "Pulse co-electrodeposition of nano Al_2O_3 whiskers nickel composite coating," *Scripta Materialia,* vol. 50, pp. 1131-1134, 2004.

[24] N. Guglielmi, "Kinetics of the Deposition of Inert Particles from Electrolytic Baths," *Journal of The Electrochemical Society,* vol. 119, pp. 1009-1012, 1972.

[25] R. K. Saha and T. I. Khan, "Effect of applied current on the electrodeposited Ni-Al_2O_3 composite coatings," *Surface and Coatings Technology,* vol. In Press, Corrected Proof.

[26] Y. L. Wang, *et al.*, "Electrodeposition and characterization of Al_2O_3-Cu(Sn), CaF_2-Cu(Sn) and talc-Cu(Sn) electrocomposite coatings," *Surface and Coatings Technology,* vol. 106, pp. 162-166, 1998.

[27] S. Arai, *et al.*, "Cu--MWCNT Composite Films Fabricated by Electrodeposition," *Journal of The Electrochemical Society,* vol. 157, pp. D147-D153, 2010.

[28] E. P. Rajiv, *et al.*, "Corrosion characteristics of cobalt-silicon nitride electro composites in various corrosive environments," *Materials Chemistry and Physics,* vol. 40, pp. 189-196, 1995.

[29] S. Hashimoto and M. Abe, "The characterization of electrodeposited Zn-SiO_2 composites before and after corrosion test," *Corrosion Science,* vol. 36, pp. 2125-2137, 1994.

[30] M. E. Bahrololoom and R. Sani, "The influence of pulse plating parameters on the hardness and wear resistance of nickel-alumina composite coatings," *Surface and Coatings Technology,* vol. 192, pp. 154-163, 2005.

[31] A. Abdel Aal, "Hard and corrosion resistant nanocomposite coating for Al alloy," *Materials Science and Engineering: A,* vol. 474, pp. 181-187, 2008.

[32] D. Thiemig, *et al.*, "Influence of pulse plating parameters on the electrocodeposition of matrix metal nanocomposites," *Electrochimica Acta,* vol. 52, pp. 7362-7371, 2007.

[33] S. A. Lajevardi and T. Shahrabi, "Effects of pulse electrodeposition parameters on the properties of Ni-TiO2 nanocomposite coatings," *Applied Surface Science,* vol. 256, pp. 6775-6781, 2010.

[34] P. Baghery, *et al.*, "Ni-TiO_2 nanocomposite coating with high resistance to corrosion and wear," *Surface and Coatings Technology,* vol. 204, pp. 3804-3810, 2010.

[35] S. W. Banovic, *et al.*, "Characterization of single and discretely-stepped electro-composite coatings of nickel-alumina," *Journal of Materials Science,* vol. 34, pp. 3203-3211, 1999.

[36] Y. Xuetao, *et al.*, "Influence of pulse parameters on the microstructure and microhardness of nickel electrodeposits," *Surface and Coatings Technology,* vol. 202, pp. 1895-1903, 2008.

[37] M. Bhardwaj, *et al.*, "Effect of current density and grain refining agents on pulsed electrodeposition of nanocrystalline nickel," *surface Engineering*, vol. In Press, Corrected Proof, 2010.

[38] X. H. Chen, *et al.*, "Electrodeposited nickel composites containing carbon nanotubes," *Surface and Coatings Technology*, vol. 155, pp. 274-278, 2002.

[39] E. Pavlatou and N. Spyrellis, "Influence of pulse plating conditions on the structure and properties of pure and composite nickel nanocrystalline coatings," *Russian Journal of Electrochemistry*, vol. 44, pp. 745-754, 2008.

[40] H. Ferkel, *et al.*, "Electrodeposition of particle-strengthened nickel films," *Materials Science and Engineering A*, vol. 234-236, pp. 474-476, 1997.

[41] D. Thiemig and A. Bund, "Characterization of electrodeposited Ni-TiO_2 nanocomposite coatings," *Surface and Coatings Technology*, vol. 202, pp. 2976-2984, 2008.

[42] T. Borkar and S. Harimkar, "Microstructure and Wear Behavior of Pulse Electrodeposited Nickel-Carbon Nanotube (Ni-CNT) Composite Coatings," *Surface Engineering*, 2010.

[43] B.-G. An, *et al.*, "Electrodeposition in the Ni-plating bath containing multi-walled carbon nanotubes," *Materials Chemistry and Physics*, vol. 110, pp. 481-485, 2008.

[44] I. Shao, *et al.*, "Synthesis and characterization of particle-reinforced Ni/Al_2O_3 nanocomposites," *Journal of Materials Research*, vol. 17, pp. 1412-1418, 2002.

[45] L. Chen, *et al.*, "Effect of surfactant on the electrodeposition and wear resistance of Ni-Al_2O_3 composite coatings," *Materials Science and Engineering: A,* vol. 434, pp. 319-325, 2006.

[46] M. R. Vaezi, *et al.*, "Electrodeposition of Ni-SiC nano-composite coatings and evaluation of wear and corrosion resistance and electroplating characteristics," *Colloids and Surfaces A: Physicochemical and Engineering Aspects,* vol. 315, pp. 176-182, 2008.

[47] W. Wang, *et al.*, "Fabrication and characterization of Ni-ZrO_2 composite nano-coatings by pulse electrodeposition," *Scripta Materialia*, vol. 53, pp. 613-618, 2005.

[48] L. Benea, "Electrodeposition and tribocorrosion behaviour of ZrO_2–Ni composite coatings," *Journal of Applied Electrochemistry,* vol. 39, pp. 1671-1681, 2009.

[49] M. Surender, *et al.*, "Wear characterization of electrodeposited Ni-WC composite coatings," *Tribology International*, vol. 37, pp. 743-749, 2004.

[50] M. Surender, *et al.*, "Electrochemical behavior of electrodeposited Ni-WC composite coatings," *Surface and Coatings Technology,* vol. 187, pp. 93-97, 2004.

[51] X. H. Chen, *et al.*, "Corrosion behavior of carbon nanotubes-Ni composite coating," *Surface and Coatings Technology,* vol. 191, pp. 351-356, 2005.

[52] W. X. Chen, *et al.*, "Tribological application of carbon nanotubes in a metal-based composite coating and composites," *Carbon*, vol. 41, pp. 215-222, 2003.

[53] S. Arai, *et al.*, "Excellent solid lubrication of electrodeposited nickel-multiwalled carbon nanotube composite films," *Materials Letters,* vol. 62, pp. 3545-3548, 2008.

[54] S. Arai, *et al.*, "Fabrication of Nickel--Multiwalled Carbon Nanotube Composite Films with Excellent Thermal Conductivity by an Electrodeposition Technique," *Electrochemical and Solid-State Letters,* vol. 9, pp. C131-C133, 2006.

[55] *Annual Book of ASTM Standars: Metals-mechanical Testings; Elevated and low temperature tests; Metallography* vol. 03.01, 2006.

[56] G. Dieter, *Mechanical Metallurgy,* 3 ed.: McGraw-Hill Companies, 1986.

[57] G.D.Hughes, *et al.*, "Hall-Petch strengthening for the microhardness of twelve nanometer grain diameter electrodeposited nickel " *Scripta Metallurgica,* vol. 20, pp. 93-97, 1986.

[58] C.P.Brittain, *et al.*, "Hall-petch dependance for ultrafine grain size electrodeposited chromium," *Sripta Metallurgica,* vol. 19, pp. 89-91, 1985.

[59] B. Szczygiel and M. Kolodziej, "Composite Ni/Al_2O_3 coatings and their corrosion resistance," *Electrochimica Acta,* vol. 50, pp. 4188-4195, 2005.

[60] A.Amadeh, *et al.*, "Corrosion Behavior of Pulse Electrodeposited Nanostructure Ni-SiC Composite Coatings " *Journal of Nanoscience and Nanotechnology,* vol. 10, pp. 5383-5388, 2010.

[61] H. S. K. G. Batis and P. Vassiliou, "Corrosion resistance of composite nickel-Al_2O_3 deposits," *Anti-Corrosion Methods and Materials,* vol. 46, pp. 29-34, 1999.

[62] I. Garcia, *et al.*, "Improved corrosion resistance through microstructural modifications induced by codepositing SiC-particles with electrolytic nickel," *Corrosion Science,* vol. 45, pp. 1173-1189, 2003.

[63] C. Guo, *et al.*, "The effects of electrodeposition current density on properties of Ni-CNTs composite coatings," *Surface and Coatings Technology,* vol. 202, pp. 3246-3250, 2008.

[64] M. Aliofkhazraei, *et al.*, "Effect of the duty cycle of pulsed current on nanocomposite layers formed by pulsed electrodeposition," *Rare Metals,* vol. 29, pp. 209-213, 2010.

[65] J. N. Balaraju and S. K. Seshadri, "Synthesis and Corrosion Behavior of Electroless Ni–P– Si_3N_4 Composite Coatings," *Journal of Materials Science Letters,* vol. 17, pp. 1297-1299, 1998.

[66] X. H. Chen, *et al.*, "Dry friction and wear characteristics of nickel/carbon nanotube electroless composite deposits," *Tribology International,* vol. 39, pp. 22-28, 2006.

[67] Z. H. Li, *et al.*, "Preparation and tribological properties of the carbon nanotubes-Ni-P composite coating," *Tribology International,* vol. 39, pp. 953-957, 2006.

[68] Y. Suzuki, *et al.*, "Electrodeposition of Ni--P Alloy--Multiwalled Carbon Nanotube Composite Films," *Journal of The Electrochemical Society,* vol. 157, pp. D50-D53, 2010.

[69] L. Benea, *et al.*, "Effect of SiC size dimensions on the corrosion wear resistance of the electrodeposited composite coating," *Materials and Corrosion,* vol. 53, pp. 23-29, 2002.

[70] M. Srivastava, *et al.*, "Influence of SiC, Si_3N_4 and Al_2O_3 particles on the structure and properties of electrodeposited Ni," *Materials Letters,* vol. 62, pp. 3487-3489, 2008.

[71] F. Erler, *et al.*, "Interface behaviour in nickel composite coatings with nano-particles of oxidic ceramic," *Electrochimica Acta,* vol. 48, pp. 3063-3070, 2003.

[72] C.-s. Chen, *et al.*, "Effect of multi-walled carbon nanotubes as reinforced fibres on tribological behaviour of Ni-P electroless coatings," *Diamond and Related Materials,* vol. 15, pp. 151-156, 2006.

[73] W. X. Chen, *et al.*, "Electroless preparation and tribological properties of Ni-P-Carbon nanotube composite coatings under lubricated condition," *Surface and Coatings Technology,* vol. 160, pp. 68-73, 2002.

[74] X. H. Chen, *et al.*, "Tribological behavior of carbon nanotubes—reinforced nickel matrix composite coatings," *Journal of Materials Science Letters,* vol. 20, pp. 2057-2060, 2001.

[75] S. R. Bakshi, *et al.*, "Carbon nanotube reinforced metal matrix composites ‐ a review," *International Materials Reviews,* vol. 55, pp. 41-64.

[76] E. J. Podlaha and D. Landolt, "Pulse-Reverse Plating of Nanocomposite Thin Films," *Journal of The Electrochemical Society,* vol. 144, pp. L200-L202, 1997.

[77] A. B. Vidrine and E. J. Podlaha, "Composite Electrodeposition of Ultrafine γ-Alumina Particles in Nickel Matrices; Part I: Citrate and chloride electrolytes," *Journal of Applied Electrochemistry,* vol. 31, pp. 461-468, 2001.

[78] T. Kuzumaki, *et al.*, "Processing of carbon nanotube reinforced aluminum composite," *Materials Research Society*, vol. 13, pp. 2445-2449, 1998.

[79] E. Flahaut, *et al.*, "Carbon nanotube-metal-oxide nanocomposites: microstructure, electrical conductivity and mechanical properties," *Acta Materialia*, vol. 48, pp. 3803-3812, 2000.

[80] C. L. Xu, *et al.*, "Fabrication of aluminum-carbon nanotube composites and their electrical properties," *Carbon,* vol. 37, pp. 855-858, 1999.

[81] Y. B. Li, *et al.*, "Physical properties of $Fe_{80}P_{20}$ glass-carbon nanotubes composite," *Journal of Materials Science,* vol. 34, pp. 5281-5284, 1999.

[82] S. R. Dong, *et al.*, "An investigation of the sliding wear behavior of Cu-matrix composite reinforced by carbon nanotubes," *Materials Science and Engineering A*, vol. 313, pp. 83-87, 2001.

[83] T. Laha, *et al.*, "Synthesis and characterization of plasma spray formed carbon nanotube reinforced aluminum composite," *Materials Science and Engineering A,* vol. 381, pp. 249-258, 2004.

[84] J. P. Tu, *et al.*, "Tribological properties of carbon-nanotube-reinforced copper composites," *Tribology Letters,* vol. 10, pp. 225-228, 2001.

[85] S. R. Bakshi, *et al.*, "Carbon nanotube reinforced aluminum composite coating via cold spraying," *Surface and Coatings Technology*, vol. 202, pp. 5162-5169, 2008.

[86] S. R. Bakshi, *et al.*, "Aluminum composite reinforced with multiwalled carbon nanotubes from plasma spraying of spray dried powders," *Surface and Coatings Technology*, vol. 203, pp. 1544-1554, 2009.

[87] J. P. Hoare, "On the Role of Boric Acid in the Watts Bath," *Journal of The Electrochemical Society*, vol. 133, pp. 2491-2494, 1986.

[88] L. Guan, *et al.*, "Exfoliation of single-walled carbon nanotube bundles under electron beam irradiation," *Carbon*, vol. 43, pp. 1101-1103, 2005.

[89] B. Zhao, *et al.*, "Synthesis and Properties of a Water-Soluble Single-Walled Carbon Nanotube–Poly(m-aminobenzene sulfonic acid) Graft Copolymer," *Advanced Functional Materials*, vol. 14, pp. 71-76, 2004.

[90] M. Tchoul, *et al.*, "Effect of Mild Nitric Acid Oxidation on Dispersability, Size, and Structure of Single-Walled Carbon Nanotubes," *Chemistry of Materials*, vol. 19, pp. 5765-5772, 2007.

[91] A. D. Krawitz, *Introduction to Diffraction in Materials Science and Engineering*: Wiley-VCH, April 2001.

[92] S. P. Harimkar and N. B. Dahotre, "Crystallographic and morphological textures in laser surface modified alumina ceramic," *Journal of Applied Physics*, vol. 100, pp. 024901-6, 2006.

[93] T. Ungár, "Microstructural parameters from X-ray diffraction peak broadening," *Scripta Materialia,* vol. 51, pp. 777-781, 2004.

APPPENDICES

Following paper was accepted and will publish very soon based on research work offered in this thesis.

Tushar Borkar and Sandip Harimkar, "Microstructure and Wear Behavior of Pulse Electrodeposited Nickel-Carbon Nanotube (Ni-CNT) Composite Coatings", Surface Engineering, 2010

VITA

Tushar Borkar

Candidate for the Degree of

Master of Science

Thesis: ELECTRODEPOSITION OF NICKEL COMPOSITE COATINGS

Major Field: Mechanical and Aerospace Engineering

Biographical:

Personal Data: Born in Pune/ India on 9th August, 1984

Education:

Completed the requirements for the Master of Science in Mechanical and Aerospace Engineering at Oklahoma State University, Stillwater, Oklahoma in December, 2010.

Completed the requirements for the Bachelor of engineering in Mechanical Engineering at Mumbai University, Mumbai, Maharashtra/INDIA in 2007.

Experience:

Graduate Research Assistant August 2008 – Present
Department of Mechanical Engineering, Oklahoma State University, Stillwater, OK, USA

Graduate Teaching Assistant August 2009 – Present
Department of Mechanical Engineering, Oklahoma State University, Stillwater, OK, USA

Lecturer August 2007 – May 2008
Department of Mechanical Engineering, Mumbai University, Mumbai, Maharashtra/INDIA

Professional Memberships: TMS, AIST, Acers, ASM, Golden Key

Name: Tushar Borkar Date of Degree: December, 2010

Institution: Oklahoma State University Location: Stillwater, Oklahoma

Title of Study: ELECTRODEPOSITION OF NICKEL COMPOSITE COATINGS

Pages in Study: 95 Candidate for the Degree of Master of Science

Major Field: Mechanical and Aerospace Engineering

Pulse electrodeposition (PC) and pulse reverse electrodeposition (PRC) bring a new era in improving the surface properties of metals. These processes are associated with many advantages, such as reduction in porosity, low level of inclusions, and higher deposition rates compared to direct current (DC) electrodeposition process. There is much more flexibility in varying three basic parameters which are, pulse current density, on time, and off time in pulse electrodeposition resulting in unique composition and microstructure of coating being deposited. In this work, nickel matrix composite coatings were synthesized by co-depositing nano particles (Al_2O_3, SiC, and ZrO_2) from Watts bath. To get detailed insight into effect of processing parameters on the microstructure, mechanical, and tribological properties of the composite coatings, the coatings were also fabricated using DC, PC, and PRC techniques. Also, the effect of bath loading on the level of reinforcement in the coating was investigated for Ni-Al_2O_3 composite coatings. Furthermore an attempt was made to produce Ni-CNT coatings by pulse electrodeposition method. Pure nickel coatings were also prepared for comparison.

Composite coatings deposited using PC and PRC techniques exhibited significant improvement in microhardness and wear resistance. The presence of nanoparticles in the composite coating seems to prohibit the columnar growth of the nickel grains resulting in random/weak texture and smaller thickness of the composite coatings. Ni-Al_2O_3 composite coatings show maximum hardness and wear resistance compared to Ni-SiC and Ni-ZrO_2 composite coatings. As Al_2O_3 content in electroplating bath increases, Microhardness and wear resistance of composite coatings increases but thickness of the coatings decreases due to nanoparticles obstructing grain growth. The Ni-CNT composite coatings exhibited significantly improved microhardness compared to pure nickel coatings.

ADVISER'S APPROVAL: Dr. Sandip P. Harimkar